The Journal of Neuroscience, August 1987, 7(8): 2373–2389

Does Mental Activity Change the Oxidative Metabolism of the Brain?

Per E. Roland,[1] Lars Eriksson,[1,2] Sharon Stone-Elander,[3] and Lennart Widen[1]

[1]Department of Clinical Neurophysiology, [2]Department of Neuroradiology, and [3]Karolinska Pharmacy, Karolinska Hospital and Institute, S-104 01 Stockholm, Sweden

Previous studies have shown that sensory stimulation and voluntary motor activity increase regional cerebral glucose consumption and regional cerebral blood flow (rCBF). The present study had 3 purposes: (1) to examine whether pure mental activity changed the oxidative metabolism of the brain and, if so, (2) to examine which anatomical structures were participating in the mental activity; and (3) to examine whether there was any coupling of the rCBF to the physiological changes in the regional cerebral oxidative metabolism ($rCMRO_2$). With a positron-emission tomograph (PET), we measured the $rCMRO_2$, rCBF, and regional cerebral blood volume (rCBV) in independent sessions lasting 100 sec each. A dynamic method was used for the measurement of $rCMRO_2$. The $rCMRO_2$, rCBF, and rCBV were measured in 2 different states in 10 young, healthy volunteers: at rest and when visually imagining a specific route in familiar surroundings. The rCBF at rest was linearly correlated to the $rCMRO_2$: rCBF (in ml/100 gm/min) = 11.4 $rCMRO_2$ + 11.9. The specific mental visual imagery increased the $rCMRO_2$ in 25 cortical fields, ranging in size from 2 to 10 cm^3, located in homotypical cortex. Active fields were located in the superior and lateral prefrontal cortex and the frontal eye fields. The strongest increase of $rCMRO_2$ appeared in the posterior superior lateral parietal cortex and the posterior superior medial parietal cortex in precuneus. Subcortically, the $rCMRO_2$ increased in neostriatum and posterior thalamus. These focal metabolic increases were so strong that the $CMRO_2$ of the whole brain increased by 10%. The rCBF increased proportionally in these active fields and structures, such that d(rCBF) in ml/100 gm/min = 11.1 d($rCMRO_2$). Thus, a dynamic coupling of the rCBF to the $rCMRO_2$ was observed during the physiological increase in neural metabolism. On the basis of previous functional activation studies and our knowledge of anatomical connections in man and other primates, the posterior medial and lateral parietal cortices were classified as remote visual-association areas participating in the generation of visual images of spatial scenes from memory, and the posterior thalamus was assumed to participate in the retrieval of such memories.

Received Aug. 26, 1986; revised Dec. 23, 1986; accepted Jan. 23, 1987.

We wish to thank Dr. Jan-Eric Litton, Göran Printz, Peter Johnström, Birgit Garmelius, Dr. Erling Nilsson, Gerd Strandlund, Charlotta Lundmark, Britt-Marie Berggren, and Monica Serrander for help during the experiments. This study was supported by grants from the Danish Medical Research Council and The Söderberg Foundation.

Correspondence should be addressed to Dr. P. E. Roland, Department of Clinical Neurophysiology, Karolinska Hospital, Box 60500, S-104 01 Stockholm, Sweden.

Mental activity is usually defined as activity that occurs in the mind alone, without any expression or sensation existing at the same time (i.e., *Chambers Twentieth Century Dictionary*). Mental activity has been the domain of classical psychology, where it has been studied by indirect methods. Neurobehavioral paradigms have included sensory stimulation and usually also motor responses. Although some mental activity is usually assumed to be interposed between the stimulus and the response, it is, in general, impossible to ascertain precisely whether cerebral events observed in this interval are consequences of the stimulus, the generation of the motor response, or due to mental activity. With very few exceptions, the physiological basis of mental activity has therefore escaped direct analysis.

From an operational point of view, mental activity is intrinsic activity of the brain in the absence of any immediate prior stimulation and of any planning and execution of motor output. If one agrees to this crude delimitation, the content of mental activity is information retrieved from the brain itself. Thinking is one type of mental activity. Thinking has been operationally defined as intrinsic activity of the brain of an awake subject who performs operations on information retrieved from the brain itself (Roland and Friberg, 1985).

Previous investigators have shown that sensory stimulation and voluntary motor activity increase the regional metabolism of the brain in animals and humans (Kennedy et al., 1976, 1980; Greenberg et al., 1979; Phelps et al., 1981; Reivich et al., 1982; Mazziotta et al., 1985). But so far, no data have appeared on pure mental activity. Some years ago, Sokoloff et al. (1955) measured the oxygen consumption of the whole brain with the Kety–Schmidt technique when subjects were at rest and when they performed mental calculations. Although the subjects both received sensory stimulation and responded with movements, Sokoloff et al. (1955) could not find any alterations of the brain oxidative metabolism. They suggested that the efficiency of the neuronal work might increase during mental activity, or that the oxidative metabolism increased in some active regions while it decreased in others, such that the net change in metabolism was zero. Recently, Roland and Friberg (1985) found that different types of thinking did indeed increase the regional cerebral blood flow (rCBF) in multiple cortical fields in such a way that the location of active fields changed with the type of thinking being performed. Roland and Friberg (1985) used the intracarotid ^{133}Xe injection technique, and thus could only measure the rCBF of the carotid-supplied part of one hemisphere. The first question that is raised in the present communication is whether one kind of specific thinking, visual imagery, would increase the oxidative metabolism of the neurons that produced this mental activity? If so, the second question was which were the anatom-

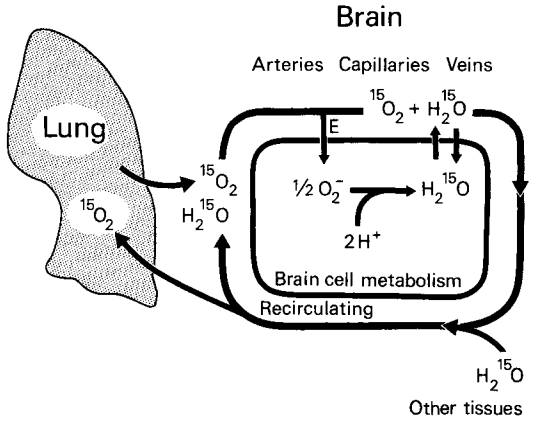

Figure 1. Oxygen extraction model. The isotope was inhaled and distributed to the brain from the arterial blood. All extraction was assumed to take place in the capillaries. The extracted ^{15}O–O_2 was assumed to be immediately metabolized into ^{15}O-water. Recirculating ^{15}O-water and ^{15}O-water produced by the metabolism were cleared by the blood flow.

ical structures participating in the retrieval of the visual images and the operations on the retrieved images?

The third question we addressed was whether any coupling existed between the regional cerebral oxidative metabolism ($rCMRO_2$) and rCBF when subjects went from rest to specific mental activity. It has been generally accepted that local changes in neuronal activity induced local changes in the neuronal metabolism which, in turn, altered the local rCBF. This view was challenged by Fox and Raichle (1986), who correctly pointed out that, with the exception of a single observation in a single neurologically abnormal individual (Raichle et al., 1976), there were no studies that determined the simultaneous effects of physiological stimulation on $rCMRO_2$ and rCBF. These authors then demonstrated that vibration of the contralateral index finger provoked a 30% increase of rCBF in the sensory hand area, which was not accompanied by any statistically significant increase of $rCMRO_2$. This uncoupling between $rCMRO_2$ and rCBF was due to the decrease of the fraction of oxygen extracted by the active neural tissue during physiological stimulation (Fox and Raichle, 1986).

The paradigm used in the present study was described by Roland and Friberg (1985): subjects visually imagined that, starting at their front door, they walked alternately to the right and the left each time they reached a corner. This mental activity was accompanied by reproducible and proportional increases in $rCMRO_2$ and rCBF in multiple cortical fields in homotypical cortex, neostriatum, and posterior thalamus.

Materials and Methods

Subjects. Ten young, normal male volunteers participated; all were between 20 and 45 years of age. Each subject gave informed consent according to the Declaration of Helsinki. None had signs, symptoms, or histories of any previous or present neurological or other disease. Nine were right-handed and one was ambidextrous according to the Edinburgh inventory (Oldfield, 1971). The study was approved by the ethics and radiation safety committees of the Karolinska Hospital.

Positron-emission tomographic measurements and measurements of the arterial radiotracer concentration. The technique of positron-emission tomography has been described in many recent publications (e.g., Greitz et al., 1985; Phelps et al., 1986).

Changes in radioactivity of the brain were monitored with a positron-emission tomograph (PET; Scanditronix PC-384-7B). The performance of this positron camera was described extensively in an earlier report (Litton et al., 1984). Briefly, the 4 detector rings, each with 96 bismuth germanate detectors, produced 7 slices of the brain, with a center-to-center distance between slices of 13.5 mm. The full-width half-maximum (FWHM) slice thickness was 11.6 mm for direct slices and 8.0 mm for cross slices in the center of the field of view. The spatial resolution (FWHM) in the plane was 8 mm. The time-coincidence window was set at 20 nsec. The response of the camera was linear up to 3 μCi/ml. In a typical study, the inhaled amount of isotope gave rise to 35,000 true coincidences/slice/sec (peak count), declining to 20,000 true coincidences/slice/sec at the end of the first 100 sec (Fig. 3). Image reconstruction, attenuation correction, corrections for scatter, and random and triple coincidences were described in earlier reports (Bergström et al., 1982; Litton et al., 1984).

The arterial radiotracer concentration was measured by an automatic sampling system (Fig. 2). A 19-gauge catheter was placed, under local anesthesia, in the left brachial artery. The device consisted of a peristaltic pump that continuously drew arterial blood from the arterial catheter past a detector consisting of a plastic scintillator. The plastic scintillator detector, which detected only positrons, was calibrated against the positron camera. A microprocessor-controlled data logger measured the arterial radiotracer concentration every second. In addition, the data logger recorded the total number of true coincidences/sec from the camera. At the end of a study, the data logger information was transferred to the host computer and written into a disk file. This file was used to (1) give a numerical output of the arterial radiotracer concentration during the study (Fig. 3); (2) give a global least-squares estimate of model parameters, such as flow, clearance, and $rCMRO_2$; and (3) give an accurate estimate of the time shift between the arterial radiotracer concentration curve and the global uptake curve from the camera (Fig. 3).

Determination of $rCMRO_2$. Determination of $rCMRO_2$ in short time intervals requires measurement of the regional oxygen-extraction fraction (E), the rCBF, and the regional cerebral blood volume (rCBV). The oxygen-extraction model is described in Figure 1. Once the rCBF and the rCBV are determined, E can be calculated:

$$E = \frac{\mathrm{PET}_0 - \mathrm{rCBF}\int_{t_1}^{t_2} \mathrm{Ca}_{H_2O}(t) * e^{-kt}\,dt - \mathrm{rCBV}\cdot R\int_{t_1}^{t_2} \mathrm{Ca}_{O_2}(t)\,dt}{\mathrm{rCBF}\int_{t_1}^{t_2} \mathrm{Ca}_{O_2}(t) * e^{-kt}\,dt - \mathrm{rCBV}\cdot R\cdot 0.835\int_{t_1}^{t_2} \mathrm{Ca}_{O_2}(t)\,dt}. \quad (1)$$

PET_0 is the total decay-corrected radiotracer activity measured by the PET camera during the total integration time (t_1,t_2) in nCi/cm^3; t_1 is the start measurement time and t_2 the stop measurement time. R is the ratio of small- to large-vessel hematocrit. The factor 0.835 is the fraction of rCBV consisting of one-half the capillary volume plus the postcapillary volume (Rushmer, 1976). The asterisk signifies a convolution operation. E was calculated pixel by pixel from this equation, introduced by Mintun et al. (1984). The determination of rCBF and rCBV was made in separate sessions (see below). Given E, the regional cerebral oxygen consumption rate is

$$\mathrm{rCMRO}_2 = E\cdot\mathrm{rCBF}\cdot\mathrm{CaO}_2, \quad (2)$$

in which CaO_2 is the amount of "cold" O_2 in the arterial blood.

For the determination of the oxygen-extraction fraction E, the subject inhaled 60 mCi of ^{15}O–O_2 (physical half-life, 123 sec) mixed in 150 ml atmospheric air in a long, smooth inhalation lasting 15 sec (Fig. 2). The inhaled ^{15}O–O_2 was transported up to the brain with the blood stream (Fig. 1). The camera's sampling of data was started when the command to expire was given to the subject. The subject expired maximally and then started the 15 second long, smooth inhalation. The sampling schedule was one scan (7 slices) every 10 sec for a total of 150 sec.

The total concentration of radiotracer in arterial blood, $\mathrm{Ca}_{tot}(t)$ was measured by the automatic blood-sampling system. After the arterial blood had passed the plastic scintillator, it was collected at 15 sec intervals in test tubes for the measurement of the ^{15}O-labeled recirculating water concentration $\mathrm{Ca}_{H_2O}(t)$ (Figs. 1, 2). The blood content in each tube was then centrifuged for 60 sec in a high-speed centrifuge. Thereafter 0.2 ml plasma was pipetted off with a Pipetman P200 R pipette (SD < 0.3 μl) and immediately measured in a well counter. The density of plasma was set to 1.02 (van Slyke et al., 1950). After decay correction, the $\mathrm{Ca}_{H_2O}(t)$ was calculated as the mean concentration in the sample interval and fitted to a third-degree polynomial times a single exponential. The fitted polynomial expression was evaluated at 1 sec intervals over the total duration of the study. We found that the amount of

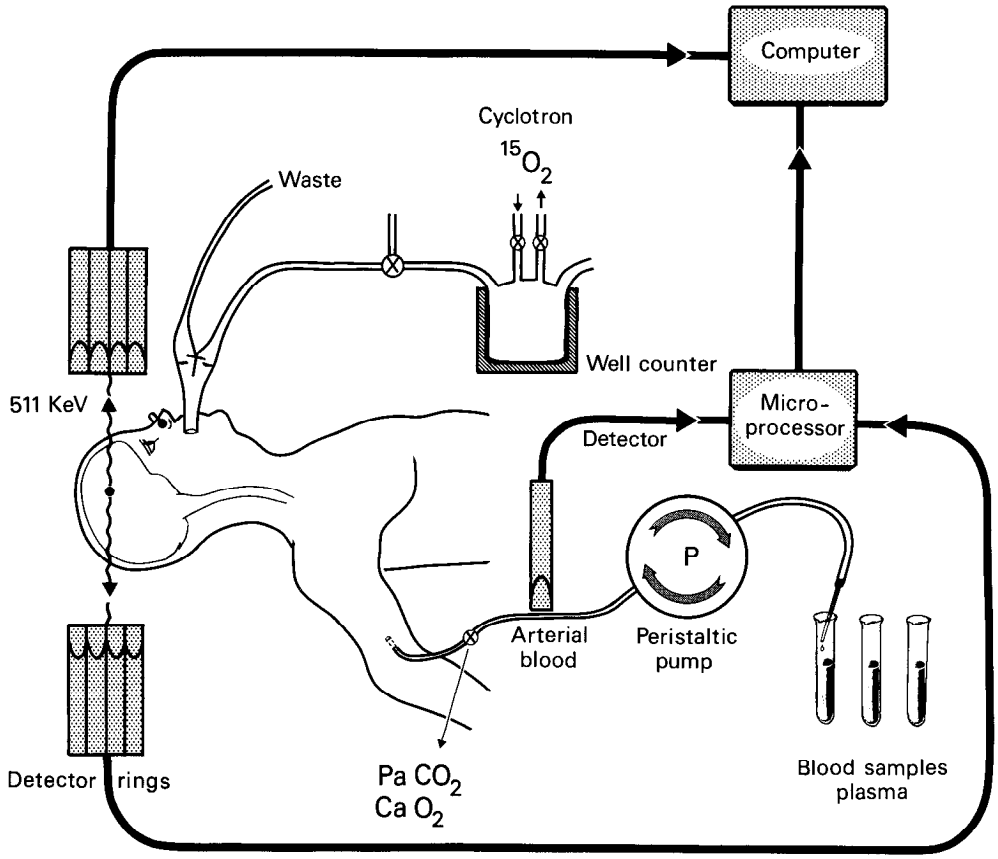

Figure 2. Measurement of the oxygen extraction. The *cyclotron* delivered ^{15}O–O_2, which was trapped in an oxygen chamber surrounded by a *well counter.* The blindfolded subject, equipped with a noseclip, inhaled 60 mCi $^{15}O_2$ in a single breath. The regional isotope concentrations in the brain were measured with a 4-ring positron emission tomograph (PET). The isotope concentration in *arterial blood* was measured continuously with an automatic blood-sampling system. *Blood samples* for determination of the partial pressure of CO_2 and the concentration of oxygen were taken through a sideline of the arterial catheter.

recirculating water increased gradually, starting some 20 sec after the start of inhalation and reaching a peak after a further 160 sec, at which time the activity was typically 1000 nCi/cm³ blood; thereafter, the activity declined slowly.

Two additional samples of arterial blood were taken with glass syringes during the first 100 sec. From these samples, the amount of "cold" oxygen, CaO_2 and $PaCO_2$, was determined. The CaO_2 was measured hemoxymetrically (Siggaard-Andersen, 1977) with an accuracy of 0.25% (SD). The rCBF in equation (1) was corrected for differences in $PaCO_2$ between rest and mental activity by 4%/mm Hg (Olesen et al., 1971). There were no systematic differences in $PaCO_2$; the largest correction factor used in this study was 1.06. The brain : blood partition coefficient for water, r_{H2O}, was needed for the determination of the oxygen extraction (equation 1). This partition coefficient was measured in a separate study by G. Blomqvist (unpublished observations), who found a value of 0.80 for the brain as a whole.

The amount of ^{15}O-labeled water in arterial blood was calculated as

$$Ca_{H_2O}(t) = C_{H_2O\ plasma}\frac{FWC_{blood}}{FWC_{plasma}}, \quad (3)$$

in which FWC_{blood} is the fractional water content of blood. From the literature, the following values are given (Davis et al., 1953): FWC_{blood} = 0.80 and FWC_{plasma} = 0.92. The $Ca_{O_2}(t)$ was then calculated by subtracting the curve for labeled recirculating water, $Ca_{H_2O}(t)$ from $Ca_{tot}(t)$.

The subjects spent 180 sec in the positron camera. From this time interval, only data from the first 90 sec (= $t_2 - t_1$) were used for the measurement of E. After 20 min, a new determination of E was made.

Measurement of the rCBF. Accurate measurement of the rCBF requires that a freely diffusible inert tracer is introduced into the brain (Kety, 1951). Therefore we have synthesized a truly inert and freely diffusible tracer, fluoromethane, ^{11}C–CH_3F, for use in rCBF measurements (Stone-Elander et al., 1986). The tracer administration was performed as follows: the oxygen container in Figure 2 was replaced by a 75 ml tube with a rubber membrane at one end. Shortly before the positron camera was started, 50 mCi ^{11}C–CH_3F in a 20 ml gas volume was injected through the rubber membrane into the tube. On the command, "expire now," the subject expired maximally and then inhaled the fluoromethane in a long, smooth inhalation lasting 15 sec. The peak radioactivity in the brain for a typical study was 23,000 true coincidences/slice/sec, declining to a minimum of 16,000 coincidences after 100 sec. Twenty sequential scans, each lasting 10 sec, were taken with the positron camera.

The arterial blood was sampled with a velocity of 2.5 ml/min by the automatic blood-sampling system (Fig. 2). The decay-corrected values of the ^{11}C–Ch_3F radiotracer concentration were stored on a computer file, together with the file of the total number of coincidences/sec from the camera. From these 2 files, the delay between the arrival of isotope to the brain and the arrival of the isotope to the scintillation crystal of the blood-activity detector was determined as described above.

From the curve of the arterial radiotracer concentration $Ca_{CH_3F}(t)$ and the PET_f (the mean local radiotracer concentration during a single scan), the rCBF was calculated pixel by pixel by the method originally described by Kety (1951). For a single scan in the time interval t_i, t_{i+1} ($t_1 < t_i$, $t_{i+1} < t_2$),

$$PET_f = \int_{t_i}^{t_{i+1}} rCBF_i Ca_{CH_3F} * e^{-kit}\, dt. \quad (4)$$

k is the clearance.

Data were obtained for a total of 200 sec, but only the first 90 sec, the interval t_1–t_2, was used for the actual computation of the rCBF. From these 90 sec of data, a whole set of corresponding values of PET_f and $Ca_{CH_3F}(t)$ were measured, from which the parameters k_i and $rCBF_i$

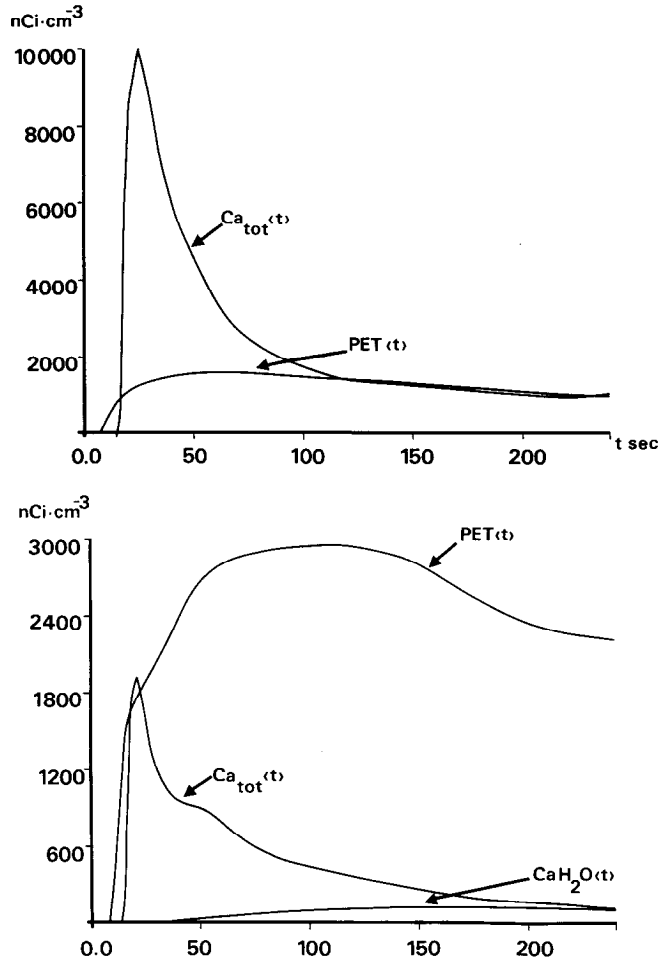

Figure 3. Top, Blood flow measurement. Curves showing $Ca_{CH_3F}(t)$, the arterial concentration of radioactive tracer (nCi/cm³ of blood), and PET(t), the total number of true coincidences from the brain (nCi/cm³ of brain). *Bottom,* Oxygen-extraction measurement. Curves showing PET(t), the total amount of radioactivity in the brain (calculated as nCi/cm³ of brain tissue); $Ca_{tot}(t)$, the total arterial radiotracer concentration (calculated as nCi/cm³ of brain tissue), and $Ca_{H_2O}(t)$, the arterial concentration of recirculating ^{15}O-water (calculated as nCi/cm³ of brain tissue). The delay between the arrival of isotope to the brain and the blood radioactivity detector is also shown.

were determined. In the actual computation of k_i, we used a maximum likelihood approach and an algorithm described by Koeppe et al. (1985). When solved for k, the brain:blood partition coefficient for $^{11}CH_3F$ was also determined. In these measurements this was found not to be significantly different from 1.0. It is also seen from Figure 3 that the brain : blood partition coefficient for $^{11}CH_3F$ is very close to 1. Thirty minutes after the start of inhalation, the brain contained less than 2% of the peak tracer concentration. A new determination of rCBF was made 60 min after the first.

Measurement of rCBV. For the measurement of rCBV, a 10 ml suspension of the subject's erythrocytes, labeled with ^{11}CO-hemoglobin (Nilsson et al., 1985) was injected intravenously. Immediately after the injection, the vein was flushed with 20 ml of physiological saline. The rCBV was calculated from scans obtained from 3 to 30 min after the start of injection:

$$\mathrm{rCBV} = \frac{100 \sum_{t_1}^{t_2} \mathrm{PET}_f}{0.85D \int_{t_1}^{t_2} \mathrm{Ca}_{CO}(t)\, dt}, \qquad (5)$$

in which PET_f, as before, was the mean local radiotracer concentration during a single scan; 0.85 was the ratio of the hematocrit in small vessels to that of large vessels (Grubb et al., 1978); D was the density of brain tissue, which was set to 1.05 gm/ml (Torack et al., 1976). The rCBV measurement was performed last, a minimum of 40 min after the start of the preceding rCBF measurement. The time interval t_1–t_2 was subdivided into periods with rest and periods with mental activity in order for us to study the effect of mental activity on the rCBV.

Behavioral control, the thinking paradigm. Twenty-four hours prior to the start of the experiments, all subjects were, with their eyes closed, trained in timing their inspiration without internal counting until they were able to do so within an interval of ±3 sec while lying connected to the actual system of administration (Fig. 2). In addition, they were trained in expiring and inspiring without any greater effort, in performing other tasks during the long inspiration, and in avoiding tensing their muscles. By the day of experimentation, all subjects were able to perform in accordance with these criteria. The subjects then had the stereotaxic helmet mounted and had 5 sham measurements prior to the actual experiments.

Each subject went through 5 measurements: 2 measurements of E (one during rest and one during mental activity), 2 meausrements of rCBF (one during rest and one during mental activity), and one measurement of rCBV. The latter measurement was subdivided into 6 periods, of which 3 were for rest and 3 were occupied with mental activity. The sequence of rest and test measurements was determined after a balanced, randomized schedule.

The reference state was called "rest." The subject was placed comfortably, supine, supported by soft pillows. He was relaxed, awake, and did not receive any stimulation. The eyes were closed with cotton wool pads and a mask to exclude light. The ears were covered by the helmet and, in addition, there was an ambient noise originating from the cooling fans of the positron camera and the wobbling mechanics. The room temperature was kept at 23°C and the light was slightly dimmed. All personnel had fixed positions and speech was prohibited. The subjects were not allowed to move, tense their muscles, to say anything or change respiratory rhythms after the inhalation. Two persons were constantly watching for muscular contractions, especially of the larynx, neck, and limbs. All subjects included were, according to these criteria, totally relaxed and motionless. The subjects were further instructed not to think of anything during rest, and especially to avoid visual images. All subjects included reported afterwards that during the rest it had been totally dark in their minds' eye.

The test paradigm and training procedures were exactly as described by Roland and Friberg (1985). In brief, when the subjects started to inspire, they imagined that they walked out their front door and then walked to the left, following the road. When they reached a road or path to the right, they imagined walking down this road; then, when a road or path opened to the left, they imagined turning down that road and so on alternatively to the right and the left each time they reached a corner in their imagined walk. The subjects were specifically instructed not to try to remember names, or to imagine their own movements during the imagined walk, but to concentrate on the *appearance of the surroundings* that they recalled in color. They should not try to correct errors if they made a wrong turn, but continue as instructed, left to right. The rationale behind this test was that, once started, the visual imagery went on in the mind of the subjects until they were stopped after 180–200 sec and asked how far they had reached. The position was then looked up on a map. Apart from the specific visual imagery and the definite operations going on in the brain, the status of the subject was exactly as during rest.

Since there was a total of 4 sessions occupied by route finding—one during the measurement of the oxygen extraction, one during the rCBF measurement, and 2 during the rCBV measurement—the subjects were instructed to imagine that they went first to the left and then to the right from the front door during the first session; first to the right and then to the left from the front door during the second session; to the left, passing the first road on the right but turning down the second to the right, and then left-right sequentially during the third session; and to the right, passing the first road to the left but turning down the second to the left, and then left to right. The subjects were never lost and unable to recall images of the surroundings. None experienced any movement of his own body.

Stereotaxic measurements and localization of metabolic activations. Each subject had a stereotaxic helmet, individually made, as described by Bergström et al. (1981). Prior to the positron scannings, each subject had a series of computer-assisted tomograms, CT scans, of the head equipped with this fixation system. Fourteen sections of the brain were

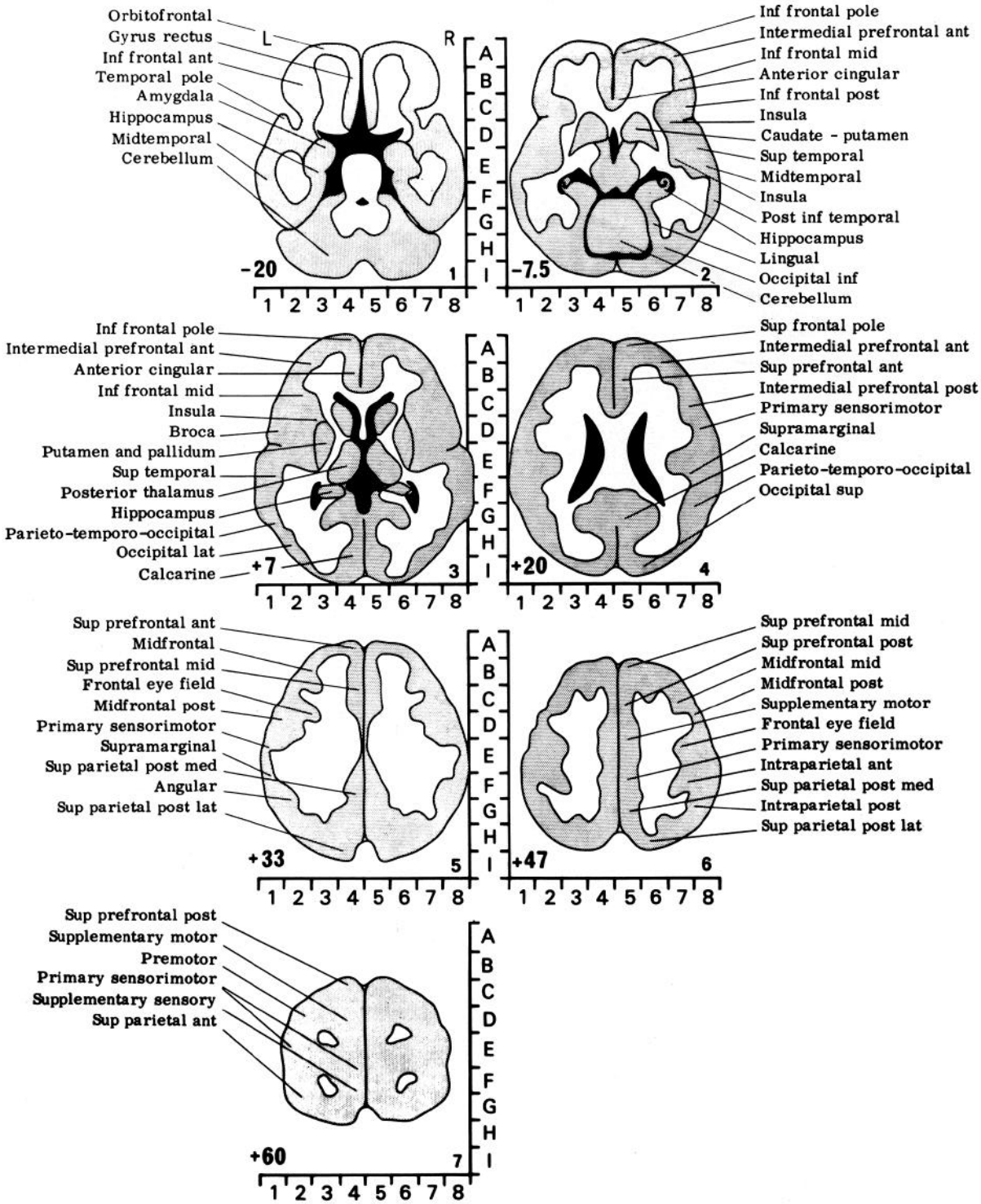

Figure 4. Atlas showing the locations of the functional subdivisions of the brain mentioned in the text and tables. The proportional stereotaxic grid system of Talairach et al. (1967) is also shown. The extension of each subdivision in stereotaxic coordinates is given in Table 5. The estimated average volume of each cortical field is shown in Tables 3 and 4. The brain was drawn with a spatial resolution like that obtained with the PET camera.

taken, of which one was the commissura anterior–commissura posterior plane. From these CT scans, a reference (z-value) was chosen for the axial positioning of the head in the positron tomograph. For all subjects, the center of the third slice of the positron tomograph was 7.0 mm above the commissural plane. The centers of the sections obtained with the positron tomograph were thus −20, −6.5, 7.0, 20.5, 34.0, 47.5, and 61.0 mm above the commissural plane. On the CT images, the brain of each subject was then proportionally subdivided into 9 frontal planes, as described by Talairach et al. (1967). The location of each horizontal section in the normalized Talairach stereotaxic box–grid system was then determined for each PET section. Since the distances between the PET sections were fixed (13.5 mm), there were small individual differences in the Talairach latitudes. The sections depicted in Figure 4 represent the mean latitudes (z-coordinates) of the 10 subjects. Each physiological change in rCBF, $rCMRO_2$, and rCBV was located to a set of Talairach coordinates (z, x, y). Since the spatial resolution in the plane

Table 1. Cerebral oxygen consumption ($CMRO_2$), cerebral blood flow (CBF), cerebral oxygen extraction (E), and cerebral blood volume (CBV) in 10 subjects at rest and when thinking. Means ± SD

	$CMRO_2$ ml/100 gm/min	CBF ml/100 gm/min	E	CBV ml/100 gm
Rest	4.00 ± 0.50	55.43 ± 6.15	0.358 ± 0.053	0.0473 ± 0.0048
Thinking	4.54 ± 0.67	59.47 ± 6.74	0.384 ± 0.050	0.0476 ± 0.0047
Difference[a]	0.63 ± 0.39[b]	4.04 ± 3.5[c]	0.02 ± 0.05	0.00045 ± 0.00103

[a] Paired comparison.
[b] $p < 0.005$.
[c] $p < 0.01$.

of the PET sections was 8 mm, Figure 4 was drawn with this resolution. Because of this limited spatial resolution, sampling of data originated from regions 8 × 8 × 11 mm^3.

The thalamus, head of the caudate, lentiform nucleus, amygdala, hippocampus, the ventricles, and the brain stem were all located in the atlas of Bohm et al. (1985). The contours of these structures were directly transferable between the CT and the PET sections.

Changes of the $rCMRO_2$, rCBF, E, and rCBV between rest and test were analyzed as follows: regions of interest (ROIs) were drawn on the $rCMRO_2$ sections in rest and during mental activity. We used the same principles of statistical delimitation as are described in Roland and Friberg (1985). In each $rCMRO_2$ section, each ROI was drawn as large as possible, but in such a way that the $rCMRO_2$ values within each ROI had a coefficient of variation <0.055 (Roland and Friberg, 1985). Within such a ROI, all pixel values could be expected to be distributed around the same mean and to have the same variance. Since the original pixel size was 2.55 × 2.55 mm, far below the spatial resolution of the camera, the variance was examined in digital maps with pixel sizes of 5.10 × 5.10 mm. From plotting the $rCMRO_2$ values within each ROI in a histogram, it was apparent that if the ROIs were drawn as described, it was reasonable to assume that the $rCMRO_2$ values within ROIs were normally distributed. All ROIs determined on the $rCMRO_2$ slices during mental activity were then transferred to the $rCMRO_2$ rest slices. In the regions delineated by the transferred ROIs, the coefficients of variation were in all cases <0.099. This meant that it was reasonable to regard the ROIs in the rest slices, as well as in the test slices, as statistically homogeneous, and calculate a mean $rCMRO_2$ for the mental activity ROI as well as the rest ROI.

Next, the $rCMRO_2$ mental activity ROIs drawn on the $rCMRO_2$ slices were transferred to the rCBF slices. Again, the coefficient of variation was examined within these transferred ROIs in the rest rCBF slices and the mental activity rCBF slices. In these cases, it was found that the coefficient of variation for all ROIs was <0.11. This meant that the ROIs in the same individual covered small regions with statistically homogeneous $rCMRO_2$ and rCBF. In order to make sure that no bias was introduced by drawing the ROIs primarily in the mental activity $rCMRO_2$ slices, we drew a net set of ROIs in the mental activity rCBF slices with the same results. The coefficient of variation after transfer for all ROIs was <0.12.

Once all ROIs were determined for all subjects, the locations of the contours were determined in the standard Talairach box–grid. ROIs occupying the same coordinates were given the same name. The coordinates, within which the average extension of the cortical ROIs were located, were then determined. The statistically homogeneous cortical ROIs were then assigned names on the basis of experiences of earlier functional mapping experiments. Throughout these experiments (see Roland and Friberg, 1985), a functional subdivision of the cortex had been obtained and mapped in the Talairach stereotaxic system. Since this functional subdivision was mapped on the surface of the brain, we delineated one region from the next by drawing borderlines perpendicular to the surface. The average cortical ROI was given the name of the region in which more than half its area was located. Although most cortical average ROIs fitted well within this subdivision, several ROIs in the occipital lobe did not. For these ROIs, new names were given and the coordinates corresponding to their average extension were listed in Table 5. It should be stressed that the ROIs were defined exclusively by their statistical homogeneity and their location. The names were only given for comparative heuristic purposes.

Thereafter, means of $rCMRO_2$s, rCBFs, Es, and rCBVs were calculated from the pixel value average for each ROI from the set drawn on the mental activity $rCMRO_2$ ROIs in each subject. On the basis of these individual means, the population means $rCMRO_2$, rCBF, E, and rCBV were calculated for each cortical ROI and each subcortical ROI (Table 3). Since each subject served as his own control, the statistical design was a paired comparison. With 92 cortical and subcortical ROIs examined in the population of 10 subjects, there was a risk that, on average, 4.5 ROIs would exceed a 2-sided significance limit of 0.05. Consequently, the significance limit for changes in $rCMRO_2$ was set at 0.005 (Tables 3 and 4).

Results

$rCMRO_2$ in normal young volunteers in rest

In rest, the subjects were awake, but not supposed to be occupied by any specific mental activity. The average $CMRO_2$ of the brain is shown in Table 1. The average metabolism does not reflect the differences in metabolism between white matter and gray matter or between different brain regions. As is seen from Table 2, the metabolism of the white matter was 1.1–1.3 ml/100 gm/min, only 25% of the metabolism of gray matter. The samples of white matter were taken from ROIs in the frontal centrum semiovale, with no ventricular space included in the ROI.

The cortex segregated into fields within which the $rCMRO_2$ was uniform. The $rCMRO_2$ values in each field were normally distributed around a mean value. The fields were distinguished on the basis of their different $rCMRO_2$ levels (Fig. 7*A*). We delineated all cortical fields and subcortical areas within which the coefficient of variation was <0.055 (see Materials and Methods). In this way 39 cortical fields were delineated in each hemisphere of each subject. If one estimates the amount of gray matter of the brain as being 700 cm^3, the average extension of the delineated 78 fields constituted 62% of the gray matter. The $rCMRO_2$ and rCBF of these cortical fields and of some subcortical structures are shown in Table 2. From Table 2 it is seen that the oxidative metabolism was high, more than 5.0 ml/100 gm/min in the superior prefrontal cortex, the calcarine cortex, and in some postparietal fields. Low $rCMRO_2$ values were seen in the posterior inferior temporal fields and the lateral occipital fields (Table 2). In these regions the cortex is thin and unfolded, and $rCMRO_2$ values were influenced by the partial volume effect (mixture of gray and white matter within the sampling space).

Within each delineated cortical field, the rCBF was also uniform. Apart from the cerebral ventricles, where the oxygen-extraction fraction was zero, the intracerebral E showed no regional variations in rest. The E of white matter was 0.34 ± 0.08, and the E of gray matter, 0.035 ± 0.06 (mean ± SD). This was in accordance with earlier findings (Frackowiak et al., 1980). Intracerebrally, the average rCBV was found to be 0.049 ± 0.005 ml/100 gm in gray matter (mean ± SD) and 0.024 ± 0.006 ml/100 gm in white matter.

Table 2. Regional cerebral oxidative metabolism and regional cerebral blood flow during rest

Region	Left hemisphere		Right hemisphere	
	$rCMRO_2$ (ml/100 gm/min)	rCBF (ml/100 gm/min)	$rCMRO_2$ (ml/100 gm/min)	rCBF (ml/100 gm/min)
Anterior cingular	5.23 ± 0.45	75.5 ± 3.3	5.37 ± 0.51	76.7 ± 3.5
Orbitofrontal	4.41 ± 0.25	58.8 ± 2.6	3.85 ± 0.19	56.2 ± 2.5
Gyrus rectus	4.98 ± 0.26	69.1 ± 3.7	5.24 ± 0.34	70.6 ± 4.0
Inferior frontal ant.	5.12 ± 0.36	67.2 ± 2.8	3.83 ± 0.39	57.3 ± 3.8
Inferior frontal mid.	4.91 ± 0.43	68.0 ± 3.9	4.46 ± 0.35	66.8 ± 3.3
Broca	4.82 ± 0.29	72.2 ± 2.8	4.76 ± 0.23	68.0 ± 2.4
Inferior frontal pole	4.35 ± 0.26	60.9 ± 3.6	4.47 ± 0.24	54.1 ± 4.0
Superior frontal pole	4.66 ± 0.31	65.0 ± 3.8	4.44 ± 0.44	62.8 ± 4.8
Intermedial prefrontal ant.	4.92 ± 0.16	64.7 ± 2.3	4.98 ± 0.16	69.2 ± 2.3
Intermedial prefrontal post.	4.87 ± 0.24	72.8 ± 3.6	4.69 ± 0.17	76.6 ± 2.7
Midfrontal ant.	4.87 ± 0.24	66.4 ± 3.4	4.74 ± 0.24	72.6 ± 3.5
Midfrontal mid.	4.96 ± 0.26	67.4 ± 2.9	5.08 ± 0.41	71.3 ± 4.6
Midfrontal post.	4.85 ± 0.22	71.9 ± 3.8	5.67 ± 0.26	78.8 ± 3.4
Frontal eye field	5.33 ± 0.20	78.2 ± 2.9	5.32 ± 0.26	76.2 ± 4.1
Superior prefrontal ant.	4.54 ± 0.22	69.5 ± 3.8	4.36 ± 0.26	72.1 ± 4.0
Superior prefrontal mid.	5.12 ± 0.30	78.4 ± 3.3	4.69 ± 0.24	74.4 ± 2.0
Superior prefrontal post.	5.34 ± 0.31	82.4 ± 3.5	5.50 ± 0.30	85.4 ± 3.2
Supplementary motor	4.76 ± 0.53	67.4 ± 3.1	5.30 ± 0.42	67.6 ± 3.1
Premotor	4.13 ± 0.41	57.2 ± 4.2	4.58 ± 0.46	63.3 ± 4.4
Primary sensory motor	4.81 ± 0.31	67.2 ± 4.1	4.81 ± 0.29	67.5 ± 3.3
Insula	5.40 ± 0.19	75.2 ± 2.9	4.64 ± 0.12	74.7 ± 3.1
Temporal pole	3.90 ± 0.31	55.3 ± 3.2	3.79 ± 0.18	52.3 ± 0.9
Superior temporal	4.83 ± 0.19	65.4 ± 2.1	4.82 ± 0.25	66.6 ± 3.0
Midtemporal	4.12 ± 0.25	55.8 ± 2.6	4.40 ± 0.19	59.9 ± 1.5
Posterior inf. temporal	3.85 ± 0.31	56.5 ± 2.9	3.76 ± 0.23	54.6 ± 2.2
Parietotemporo-occipital	4.29 ± 0.32	59.4 ± 3.2	4.72 ± 0.18	60.7 ± 2.1
Lingual	4.11 ± 0.46	57.8 ± 2.8	4.36 ± 0.21	57.2 ± 2.9
Calcarine	5.12 ± 0.32	66.9 ± 3.5	5.04 ± 0.23	61.4 ± 2.3
Occipital inf.	3.62 ± 0.58	56.1 ± 2.8	3.90 ± 0.46	50.0 ± 6.6
Occipital lat.	4.07 ± 0.27	51.6 ± 3.1	3.83 ± 0.25	49.0 ± 3.4
Occipital sup.	4.49 ± 0.21	51.5 ± 2.2	4.36 ± 4.63	53.2 ± 2.8
Supplementary sensory	4.99 ± 0.30	65.7 ± 2.9	5.30 ± 0.42	65.4 ± 3.2
Superior parietal ant.	4.64 ± 0.54	58.1 ± 5.6	4.68 ± 0.56	63.9 ± 6.9
Intraparietal ant.	5.52 ± 0.46	68.2 ± 4.0	5.70 ± 0.33	68.9 ± 2.7
Intraparietal post.	5.32 ± 0.29	64.3 ± 3.3	5.16 ± 0.19	64.7 ± 2.6
Supramarginal	4.88 ± 0.20	67.9 ± 4.0	4.96 ± 0.31	73.5 ± 3.2
Angular	4.79 ± 0.31	64.8 ± 3.3	4.78 ± 0.35	60.0 ± 4.5
Superior parietal post. med.	5.99 ± 0.44	75.3 ± 4.0	5.85 ± 0.34	73.0 ± 3.0
Superior parietal post. lat.	5.54 ± 0.49	69.8 ± 3.7	5.06 ± 0.25	64.2 ± 2.8
White matter	1.25 ± 0.16	20.0 ± 0.6	1.09 ± 0.07	20.0 ± 1.8
Hippocampus	3.18 ± 0.37	58.5 ± 3.7	3.65 ± 0.23	57.0 ± 2.6
Caput caudatus	3.71 ± 0.29	55.7 ± 6.1	3.84 ± 0.36	67.5 ± 3.6
Caudatus-putamen	4.32 ± 0.19	66.0 ± 2.2	4.61 ± 0.25	64.2 ± 4.5
Putamen-pallidum	5.05 ± 0.32	67.5 ± 5.0	5.01 ± 0.30	68.4 ± 4.6
Thalamus	3.18 ± 0.37	73.0 ± 3.1	4.75 ± 0.27	67.6 ± 5.0
Cerebellum	4.55 ± 0.31	59.8 ± 2.4	4.17 ± 0.10	58.0 ± 2.5

Changes in $rCMRO_2$ and rCBF induced by thinking

The first question was whether thinking would change the overall metabolism of the brain. Table 1 gives the normal values of $CMRO_2$ and CBF during thinking. Since the design was a paired comparison in which each subject served as his own control, a stronger statistic was applied for the paired individual differences (t test). Thinking then produced a clear increase in $CMRO_2$ and CBF of the whole brain (Table 1). This increase in the metabolism of the brain was caused by increaes of $rCMRO_2$ and rCBF in 25 cortical fields and 4 subcortical structures (Tables 3, 4). In Tables 3 and 4 it is also seen that there were no significant decreases in the local metabolism when the subjects went from rest to thinking. The increases in $rCMRO_2$ thus were

Table 3. Changes in regional cerebral oxygen consumption ($rCMRO_2$), regional cerebral blood flow (rCBF), oxygen extraction fraction (*E*), and regional cerebral blood volume (rCBV) in the *right* hemisphere of 10 thinking subjects (means ± SE)

Region	Size (cm^3)	$rCMRO_2$ (ml/100 gm/min)	rCBF (ml/100 gm/min)	*E*	rCBV (ml/100 gm)
Anterior cingular	4.4 ± 0.8	0.27 ± 0.17	4.4 ± 3.2	0.04 ± 0.05	0.009 ± 0.006
Orbitofrontal	9.2 ± 1.6	0.58 ± 0.17	6.3 ± 2.6	0.00 ± 0.02	0.006 ± 0.003
Gyrus rectus	7.2 ± 1.2	0.66 ± 0.42	6.7 ± 4.7	−0.01 ± 0.04	0.001 ± 0.004
Inferior frontal ant.	6.1 ± 0.9	0.77 ± 0.43	9.4 ± 2.3[b]	0.02 ± 0.04	−0.001 ± 0.005
Inferior frontal mid.	4.1 ± 0.7	0.35 ± 0.18	2.0 ± 3.9	0.02 ± 0.02	0.001 ± 0.002
Inferior frontal post.	4.6 ± 0.6	0.11 ± 0.18	8.6 ± 2.8	−0.02 ± 0.02	0.005 ± 0.003
Inferior frontal pole	3.7 ± 0.6	0.61 ± 0.25	6.8 ± 1.0[a]	0.01 ± 0.02	0.004 ± 0.005
Superior frontal pole	2.9 ± 0.4	0.69 ± 0.20	11.1 ± 3.5	0.01 ± 0.02	0.000 ± 0.002
Intermedial prefrontal ant.	9.5 ± 1.1	1.07 ± 0.21[a]	10.6 ± 0.7[a]	0.04 ± 0.02	0.003 ± 0.001
Intermedial prefrontal post.	4.4 ± 0.6	1.28 ± 0.19[a]	9.6 ± 1.9[a]	0.03 ± 0.01	0.006 ± 0.001
Midfrontal ant.	4.1 ± 0.5	1.42 ± 0.27[a]	11.3 ± 2.5[b]	0.04 ± 0.02	0.000 ± 0.002
Midfrontal mid.	3.3 ± 0.7	1.48 ± 0.33[b]	17.4 ± 2.9[a]	0.03 ± 0.02	0.002 ± 0.001
Midfrontal post.	4.5 ± 0.9	0.96 ± 0.38	7.6 ± 2.0	0.02 ± 0.02	0.003 ± 0.002
Frontal eye field	2.3 ± 0.4	1.20 ± 0.33	12.2 ± 2.5[b]	0.03 ± 0.02	0.003 ± 0.004
Superior prefrontal ant.	5.0 ± 0.9	1.17 ± 0.33[b]	11.2 ± 2.2[a]	0.02 ± 0.02	0.004 ± 0.003
Superior prefrontal mid.	4.2 ± 0.5	1.34 ± 0.19[a]	15.4 ± 3.4[b]	0.04 ± 0.02	0.004 ± 0.007
Superior prefrontal post.	5.6 ± 0.7	0.14 ± 0.29[b]	7.4 ± 1.8[b]	0.04 ± 0.01	0.001 ± 0.002
Supplementary motor	5.2 ± 0.7	0.55 ± 0.35	4.6 ± 4.1	0.03 ± 0.05	0.004 ± 0.004
Premotor	3.8 ± 0.5	0.39 ± 0.23	3.8 ± 1.9	0.00 ± 0.02	0.002 ± 0.002
Primary sensorimotor	18.2 ± 1.6	0.30 ± 0.13	3.3 ± 2.8	0.01 ± 0.02	−0.001 ± 0.002
Insula	7.0 ± 0.6	0.82 ± 0.26	8.5 ± 2.9	0.02 ± 0.01	0.003 ± 0.001
Temporal pole	6.2 ± 1.0	0.62 ± 0.21	9.4 ± 3.9	0.00 ± 0.02	0.005 ± 0.002
Superior temporal	5.4 ± 0.6	0.95 ± 0.29	11.0 ± 2.5[b]	0.02 ± 0.01	0.004 ± 0.001
Midtemporal	3.0 ± 0.3	0.42 ± 0.17	7.5 ± 2.6	0.00 ± 0.02	0.001 ± 0.001
Posterior inf. temporal	3.8 ± 0.3	0.47 ± 0.12[b]	10.2 ± 2.3[b]	−0.01 ± 0.02	0.000 ± 0.002
Parietotemporo-occipital	5.7 ± 0.7	0.48 ± 0.18	6.1 ± 3.5	0.01 ± 0.02	−0.001 ± 0.002
Lingual	4.0 ± 0.5	0.81 ± 0.34	10.2 ± 4.4	0.02 ± 0.03	0.003 ± 0.002
Calcarine	8.4 ± 0.3	0.70 ± 0.30	10.0 ± 2.8	−0.03 ± 0.02	0.003 ± 0.003
Occipital inf.[c]	4.1 ± 0.5	0.62 ± 0.19	8.7 ± 2.4	0.00 ± 0.02	0.002 ± 0.002
Occipital lat.[c]	5.6 ± 0.8	0.38 ± 0.10	5.2 ± 1.7	0.01 ± 0.02	−0.004 ± 0.004
Occipital sup.	5.2 ± 0.8	0.51 ± 0.13[b]	9.7 ± 1.8[a]	−0.01 ± 0.02	0.003 ± 0.004
Supplementary sensory	4.3 ± 0.8	0.49 ± 0.31	5.4 ± 3.9	0.02 ± 0.02	0.000 ± 0.002
Superior parietal ant.	4.1 ± 0.3	0.39 ± 0.26	1.9 ± 4.1	0.02 ± 0.02	0.000 ± 0.003
Intraparietal ant.	4.5 ± 0.4	0.67 ± 0.16[b]	10.2 ± 3.6	0.03 ± 0.02	0.001 ± 0.001
Intraparietal post.	4.0 ± 0.3	1.30 ± 0.21[a]	14.4 ± 2.3[a]	0.015 ± 0.01	0.001 ± 0.002
Supramarginal	7.9 ± 1.4	1.15 ± 0.22[a]	9.1 ± 1.8[a]	0.03 ± 0.02	−0.001 ± 0.001
Angular	2.9 ± 0.7	0.39 ± 0.20	7.4 ± 3.8	−0.01 ± 0.03	0.003 ± 0.002
Superior parietal post. med.	6.2 ± 1.0	1.30 ± 0.31[b]	13.7 ± 2.8[b]	0.00 ± 0.02	−0.002 ± 0.003
Superior parietal post. lat.	5.5 ± 0.5	1.48 ± 0.32[a]	12.6 ± 2.2[a]	0.03 ± 0.02	0.000 ± 0.003
White matter	4.8 ± 0.9	0.07 ± 0.15	−1.4 ± 1.4	0.03 ± 0.04	0.001 ± 0.002
Hippocampus[c]	2.9 ± 0.6	0.55 ± 0.38	7.5 ± 2.6	−0.02 ± 0.02	0.003 ± 0.004
Caput caudatus	1.5 ± 0.2	1.04 ± 0.21[a]	10.5 ± 1.8[a]	0.04 ± 0.03	0.005 ± 0.004
Caudatus-putamen	3.2 ± 0.3	1.15 ± 0.22[a]	8.8 ± 1.5[a]	0.03 ± 0.02	0.000 ± 0.002
Putamen-pallidum	3.4 ± 0.4	1.03 ± 0.20[a]	15.5 ± 2.7[a]	0.00 ± 0.02	−0.000 ± 0.002
Thalamus	2.7 ± 0.3	1.23 ± 0.27[a]	15.1 ± 3.9[b]	0.01 ± 0.02	−0.002 ± 0.003
Cerebellum	12.0 ± 2.0	0.94 ± 0.16[a]	8.9 ± 2.4	0.02 ± 0.02	0.002 ± 0.002

[a] $p < 0.001$.

[b] $p < 0.005$; *t* test paired comparison.

[c] Region with partial volume effect.

not compensated for by decreases in $rCMRO_2$ elsewhere.

The cortical fields, which had a statistically homogeneous $rCMRO_2$ during thinking, also had a statistically homogeneous rCBF during thinking (coefficient of variation <0.10) and vice versa (Fig. 7, *C, D*). Furthermore, the fields that had a homogeneous $rCMRO_2$ at rest also had a homogeneous rCBF at rest (coefficient of variation <0.11). This held true for all 78 cortical fields listed in Tables 3 and 4. Furthermore, rCBF increased over the whole field during thinking, as earlier described by Roland and Friberg (1985). The new finding was that both $rCMRO_2$ and rCBF increased over the whole field during physiological brain work.

Table 4. Changes in regional cerebral oxygen consumption ($rCMRO_2$), regional cerebral blood flow (rCBF), oxygen extraction fraction (E), and regional cerebral blood volume (rCBV) in the *left* hemisphere of the thinking subjects (means ± SE)

Region	Size (cm^3)	$rCMRO_2$ (ml/100 gm/min)	rCBF (ml/100 gm/min)	E	rCBV (ml/100 gm)
Anterior cingular	4.7 ± 0.7	0.37 ± 0.31	6.3 ± 2.4	0.05 ± 0.04	0.002 ± 0.006
Orbitofrontal	9.0 ± 1.5	0.71 ± 0.35	8.4 ± 3.7	0.00 ± 0.03	−0.001 ± 0.002
Gyrus rectus	7.3 ± 1.1	0.32 ± 0.32	3.3 ± 3.7	−0.02 ± 0.04	0.001 ± 0.001
Inferior frontal ant.	4.0 ± 0.6	0.33 ± 0.24	11.6 ± 5.6	0.02 ± 0.05	0.002 ± 0.004
Inferior frontal mid.	3.6 ± 0.8	0.21 ± 0.13	3.2 ± 2.0	−0.01 ± 0.02	0.001 ± 0.001
Broca	5.2 ± 0.7	0.79 ± 0.29	6.8 ± 2.9	0.01 ± 0.02	0.005 ± 0.003
Inferior frontal pole	3.9 ± 0.5	0.62 ± 0.19	6.8 ± 1.6[b]	0.01 ± 0.02	−0.006 ± 0.004
Superior frontal pole	3.1 ± 0.3	0.49 ± 0.18	5.8 ± 2.8	0.01 ± 0.03	0.002 ± 0.001
Intermedial prefrontal ant.	7.7 ± 1.5	1.01 ± 0.18[a]	11.9 ± 1.8[a]	0.01 ± 0.02	0.001 ± 0.002
Intermedial prefrontal post.	4.2 ± 0.6	0.93 ± 0.14[a]	14.2 ± 2.1[a]	0.01 ± 0.01	0.001 ± 0.002
Midfrontal ant.	5.0 ± 0.7	1.04 ± 0.22[b]	18.3 ± 5.1	0.01 ± 0.02	−0.004 ± 0.003
Midfrontal mid.	4.3 ± 0.7	0.54 ± 0.15	6.9 ± 3.0	0.01 ± 0.02	0.004 ± 0.009
Midfrontal post.	4.5 ± 0.9	1.50 ± 0.21[a]	14.3 ± 2.1[a]	0.03 ± 0.02	0.001 ± 0.003
Frontal eye field	2.3 ± 0.2	0.96 ± 0.15[a]	7.7 ± 1.8[b]	0.02 ± 0.01	−0.009 ± 0.006
Superior prefrontal ant.	4.1 ± 0.7	1.16 ± 0.25[b]	7.4 ± 2.3	0.07 ± 0.04	0.005 ± 0.003
Superior prefrontal mid.	4.1 ± 0.7	0.82 ± 0.25	11.4 ± 2.4[a]	0.01 ± 0.01	0.002 ± 0.002
Superior prefrontal post.	4.8 ± 0.7	1.47 ± 0.34[b]	9.8 ± 2.5[b]	0.04 ± 0.01	−0.001 ± 0.002
Supplementary motor	5.1 ± 0.8	0.56 ± 0.36	4.6 ± 4.1	0.03 ± 0.02	0.004 ± 0.004
Premotor	3.4 ± 0.5	0.53 ± 0.11	3.2 ± 2.4	−0.03 ± 0.02	0.002 ± 0.003
Primary sensorimotor	17.1 ± 1.3	0.38 ± 0.18	3.2 ± 3.1	0.01 ± 0.02	0.000 ± 0.000
Insula	5.8 ± 0.7	1.24 ± 0.34	16.6 ± 2.8[a]	−0.00 ± 0.02	0.000 ± 0.002
Temporal pole	5.5 ± 0.8	0.99 ± 0.33	6.2 ± 2.2	0.04 ± 0.02	−0.001 ± 0.004
Superior temporal	5.3 ± 0.6	0.66 ± 0.21	7.5 ± 7.7	0.03 ± 0.02	0.003 ± 0.004
Midtemporal	2.5 ± 0.2	0.57 ± 0.20	6.2 ± 2.6	−0.00 ± 0.02	0.004 ± 0.003
Posterior inf. temporal[c]	4.1 ± 0.4	0.60 ± 0.19	8.3 ± 1.8[b]	0.01 ± 0.02	−0.001 ± 0.002
Parietotemporo-occipital	4.9 ± 0.7	0.53 ± 0.09[a]	7.5 ± 2.3	−0.01 ± 0.02	0.004 ± 0.003
Lingual	2.9 ± 0.3	0.86 ± 0.23	11.5 ± 2.8	0.01 ± 0.03	−0.003 ± 0.005
Calcarine	4.3 ± 0.6	0.90 ± 0.35	5.1 ± 2.6	0.02 ± 0.03	0.002 ± 0.003
Occipital inf.[c]	3.3 ± 0.5	0.64 ± 0.31	12.3 ± 3.5[d]	−0.02 ± 0.03	0.003 ± 0.003
Occipital lat.[c]	5.0 ± 0.7	0.33 ± 0.26	3.0 ± 4.0	0.00 ± 0.03	−0.002 ± 0.006
Occipital sup.	4.8 ± 0.9	0.68 ± 0.17	12.2 ± 1.8[a]	−0.03 ± 0.03	0.003 ± 0.002
Supplementary sensory	3.7 ± 0.8	0.79 ± 0.31	5.5 ± 3.9	0.03 ± 0.01	0.000 ± 0.002
Superior parietal ant.	3.3 ± 0.4	0.78 ± 0.28	4.7 ± 4.1	0.02 ± 0.03	0.001 ± 0.003
Intraparietal ant.	3.5 ± 0.7	0.44 ± 0.17	8.5 ± 2.1[b]	−0.02 ± 0.02	0.001 ± 0.001
Intraparietal post.	4.1 ± 0.5	1.15 ± 0.19[a]	15.4 ± 1.6[a]	−0.01 ± 0.01	0.002 ± 0.002
Supramarginal	5.0 ± 1.0	0.76 ± 0.21	10.2 ± 2.4[b]	0.01 ± 0.03	0.002 ± 0.002
Angular	3.4 ± 0.4	0.88 ± 0.15	10.8 ± 3.0	0.01 ± 0.02	0.002 ± 0.002
Superior parietal post. med.	5.7 ± 0.7	1.34 ± 0.31[b]	15.5 ± 3.0[a]	0.01 ± 0.01	0.007 ± 0.007
Superior parietal post. lat.	4.8 ± 0.8	1.43 ± 0.30[b]	11.0 ± 2.3[a]	0.04 ± 0.02	−0.000 ± 0.002
White matter	4.1 ± 0.7	−0.10 ± 0.14	0.3 ± 0.7	−0.04 ± 0.04	0.003 ± 0.002
Hippocampus[c]	2.4 ± 0.8	0.56 ± 0.34	9.8 ± 3.2	0.00 ± 0.03	0.002 ± 0.003
Caput caudatus	1.2 ± 0.2	0.40 ± 0.27	16.1 ± 4.0[b]	−0.07 ± 0.06	0.003 ± 0.005
Caudatus-putamen	2.9 ± 0.2	0.97 ± 0.21[b]	11.4 ± 1.4[a]	0.03 ± 0.02	0.001 ± 0.002
Putamen-pallidum	2.7 ± 0.2	0.95 ± 0.17[a]	13.5 ± 3.7	0.01 ± 0.03	0.006 ± 0.004
Thalamus	2.9 ± 0.2	1.10 ± 0.25[b]	12.0 ± 2.7[b]	0.01 ± 0.03	−0.007 ± 0.006
Cerebellum	8.8 ± 1.0	1.07 ± 0.40	11.2 ± 2.3[a]	0.02 ± 0.01	−0.000 ± 0.002

[a] $p < 0.001$.
[b] $p < 0.005$; t test paired comparison.
[c] Region with partial volume effect.
[d] $n = 5$.

Coupling of rCBF to $rCMRO_2$

When the mean $rCMRO_2$s for each of the 78 delineated cortical fields and 14 subcortical structures were plotted versus the mean rCBF in the same fields and structures during rest, there was a linear correlation between the mean $rCMRO_2$ and the mean rCBF (Fig. 5). This linear correlation also held true for the $rCMRO_2$ and rCBF in the individual subject. This was in accordance with the findings of Carter et al. (1972) and Baron et al. (1982).

The finding of clear increases of rCBF and $rCMRO_2$ during thinking argued against uncoupling between the rCBF and the

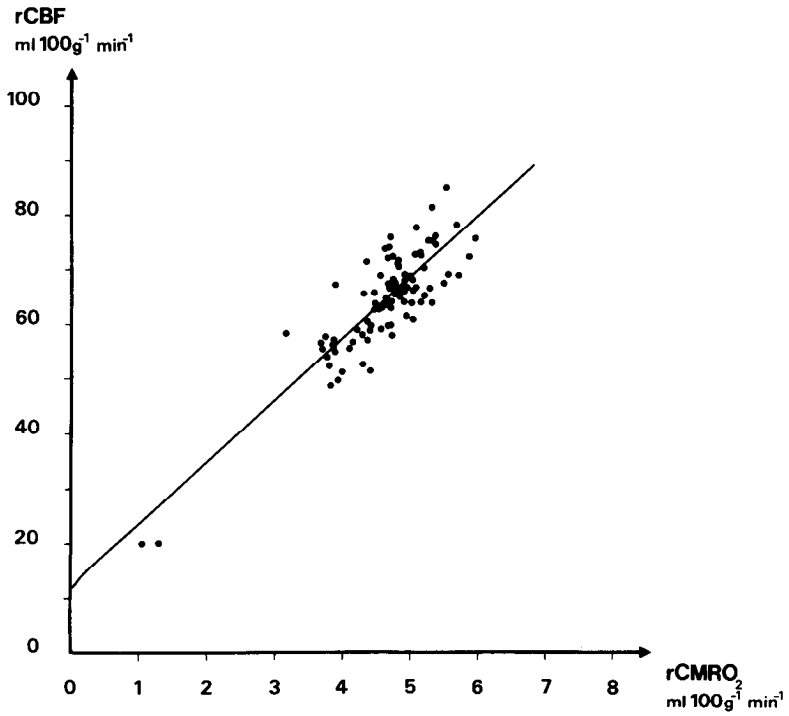

Figure 5. Mean $rCMRO_2$ in rest from 39 cortical fields, 6 subcortical structures, and the white matter in the right and left hemispheres plotted against the mean rCBF in the same structures. The equation for the linear regression was $rCBF = 11.39rCMRO_2 + 11.92$; correlation coefficient, $r = 0.859$; $p < 0.001$. Ten subjects.

$rCMRO_2$, as found by Fox and Raichle (1986) during sensory stimulation. If the rCBF increased without any significant increase in $rCMRO_2$, the oxygen extraction would decrease in the active fields and structures. However, Tables 3 and 4 clearly show no significant changes of E when the brain went from rest to physiological brain work, thinking. Neither could we find any changes of the intracerebral rCBV. In contrast, within each active field and structure there were proportional increases in rCBF and $rCMRO_2$ (Tables 3, 4). When the change in rCBF was plotted against that in $rCMRO_2$ for each delineated cortical field and subcortical structure, the correlation between the ΔrCBF and $\Delta rCMRO_2$ was clearly linear (Fig. 6). The slope of the linear regression in Figure 6 is 11.11, which is not significantly different from the slope, 11.39, of the regression between rCBF and $rCMRO_2$ obtained during rest ($0.990 < p < 0.995$). In other words, differentiation of the equation that describes the relation between rCBF and $rCMRO_2$ at rest yielded the equation for the rCBF–$rCMRO_2$ regression during physiological brain work: $d(rCBF) = 11.1\ d(rCMRO_2)$. This meant that in the brain the rCBF and the $rCMRO_2$ had the same linear correlation in rest as during physiological brain work.

Since the rCBF increased in many cortical fields above 25%, it might seem strange that the rCBV within the same regions did not change. The cortical increases in rCBF were largest in slice 6 (Fig. 7). We delineated the extracerebral space in slice 6 for which rCBV > 0.05 in rest. This space, which mainly consisted of venules and cerebrospinal fluid, increased its rCBV during thinking by 7.3 ± 1.7% ($p < 0.01$). This meant that presumably the venules and veins draining the cortical fields having the greatest increases in rCBF increased their blood volume, whereas the intracerebral rCBVs within the most active fields did not change to any measurable extent (Fig. 7, *C, E*). We found no systematic changes in $PaCO_2$ ($p > 0.2$) or oxygen content in arterial blood CaO_2 ($p > 0.2$) between rest and thinking.

Localization of the $rCMRO_2$ changes

The mental activity, thinking, comprised, first, a retrieval of a series of previously stored images of the familiar surroundings. Contingent on the spatial information in the recalled image, a new set of visual images had to be recalled. This retrieval and operations on the retrieved images increased the $rCMRO_2$ in 25 cortical fields located outside the primary sensory cortices and the motor cortices (Tables 3, 4; Fig. 7). The localizations of all active cortical fields are shown in Figure 4. In Table 5, the average extensions of all cortical fields, active and inactive, mentioned in the text and the tables are given in stereotaxic coordinates. In the *anterior* part of the brain, the active cortical fields occupied most of the superior prefrontal cortex and midsection and intermedial section of the prefrontal cortex (Fig. 7, *A, B*). In addition, the left frontal eye field increased its $rCMRO_2$.

In the *posterior* part of the brain, the following cortical regions showed fields of increased $rCMRO_2$: the supramarginal cortex; the cortex lining the intraparietal sulcus, especially the posterior part; the right posterior inferior temporal cortex; the left parietotemporo-occipital cortex; the superior occipital cortex on the lateral side of the occipital lobe; and the posterior superior parietal cortex, which had the 2 fields showing the largest increases in $rCMRO_2$, 1.3–1.6 ml/100 gm/min (Tables 3, 4). In one of these 2 fields, the lateral field on the lateral side of the superior parietal lobule, the activated areas were confined to slices 5 and 6, with approximately the same extension in all individuals (Fig. 7, *A, B*). The medial field extended from the calcarine cortex up to the superolateral border of the hemisphere, comprising slices 4, 5, and 6 in most subjects (Fig. 7*B*). It is, however, possible that this region consists of 2 functionally different parts, because the increase of $rCMRO_2$ in 4 subjects was confined to slices 5 and 6 alone. The area just in front of the calcarine cortex in the medial side of the hemisphere showed strong $rCMRO_2$ increases in some, but not all, subjects. With the limited spatial

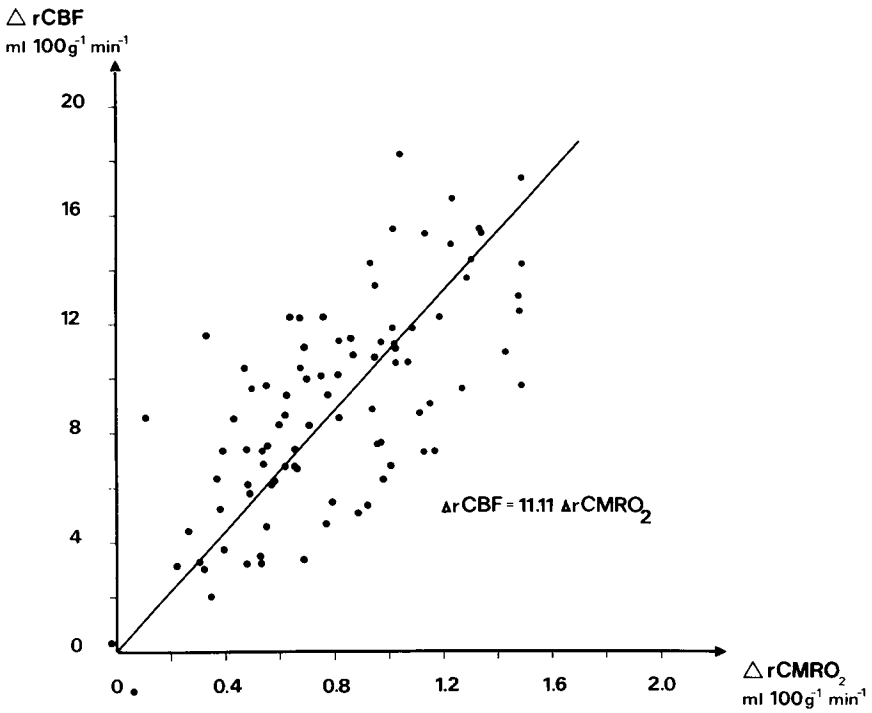

Figure 6. Plot of the mean change in rCBF, ΔrCBF, versus the mean change in $rCMRO_2$, $\Delta rCMRO_2$, induced by thinking. Results are shown for the same 78 cortical fields and 12 subcortical structures as are depicted in Figure 5. Analysis of the regression gave a straight line with an intercept not significantly different from (0,0) ($p < 0.3$). The regression equation was $\Delta rCBF = 11.11 \Delta rCMRO_2$ ($r = 0.620$; $p < 0.001$).

resolution of the positron camera, we were not able to distinguish the functional differences in this folded cortex around the isthmus of the cingular gyrus. The calcarine cortex did not increase its metabolism (Tables 3, 4; Fig. 7); neither did the cortex immediately lateral and inferior to the calcarine cortex.

Subcortically, $rCMRO_2$ increased in the head of the right caudate nucleus, bilaterally in neostriatum (caudate-putamen), and thalamus. The caudate-putamen appeared in slice 2 as one structure. The same was true for putamen and a minor part of pallidum in slice 3. Therefore, there was no possibility of determining exactly where the $rCMRO_2$ increase had originated. According to the stereotaxic measurements and the atlas of Bohm et al. (1985), the $rCMRO_2$ increases in the 2 thalami were located to the posterior parts (Fig. 7*B*). In addition, the right lateral cerebellar hemisphere was activated.

Subjects' report of their imagined walks

When the distance the subjects had covered in their internal "walks," was looked up on a map, we found that during the 150 sec they were thinking, the subjects changed direction 5.4 ± 2.5 times (mean ± SD) and covered a distance of 1160 ± 742 m. It was not possible to correlate these values with the $rCMRO_2$ increases of any region in the parietal or occipital cortex. All subjects reported that there were almost no "black periods" in which the visual imagery disappeared, or in which they had difficulties retrieving a subsequent scene. All subjects imagined the recalled sceneries in color, often vividly linked to situations. One stopped for a red light, another remembered the colors of parked cars. All subjects imagined themselves walking in the center of a 3-dimensional colored space. They described the spatial relations as those of the real world, but, in addition, they were able to look around in the 3-dimensional scenery and were capable of zooming in on certain details in the scenery as well.

Discussion

The main new findings were that mental activity increased the oxidative metabolism of the brain, and that this increase, in turn, was due to increases in the regional oxidative metabolic rate in a particular set of multiple cortical fields, thalamus and neostriatum. Within each activated field, the rCBF was linearly coupled to the $rCMRO_2$. The correlation data indicated that the same coupling exists in rest as well as during physiological activity.

Comments on methods

The $rCMRO_2$ was calculated according to a new model introduced by Mintun et al. (1984). The model had very few limiting assumptions. One was that all extracted oxygen was immediately metabolized into water, leaving no free extramitochondrial oxygen in the brain tissue. This is obviously wrong, as was also pointed out by Mintun et al. (1984), because some oxygen must be traveling from the hemoglobin to the cytochrome, or there would be no oxidative metabolism at all. However, direct measurements of the oxygen tension in the brain tissue have shown tensions between 1 mm Hg and 5 mm Hg (Silver, 1966; Lubbers, 1974). The solubility of oxygen in brain tissue is low (Thews, 1960). The error of neglecting the free tissue oxygen was estimated to be less than 2%.

Another error would arise if not all of the oxygen extracted was turned into water. In the brain there are some enzymes, such as cytochrome P-450, tyrosine hydroxylase, phenylalanine hydroxylase, and tryptophan hydroxylase, that are able to bind $^{15}O_2$. The amount of these enzymes and the slowness of their turnover rate in comparison with that of the cytochromes of the respiratory chain indicate that less than 1% of the labeled oxygen would be bound to the substrates of these enzymes (Friedman et al., 1972).

Another assumption was that the arterial oxygen consumption instantaneously influenced the capillary and postcapillary concentration. Since the cerebral transit time for the isotope is short—1–2 sec (Greitz, 1956)—compared to the total integration time—t_1–t_2 of 90 sec—our approximation was considered of no practical importance for normal subjects (Huang et al., 1986). The estimated values of $rCMRO_2$ and rCBF were quite sensitive

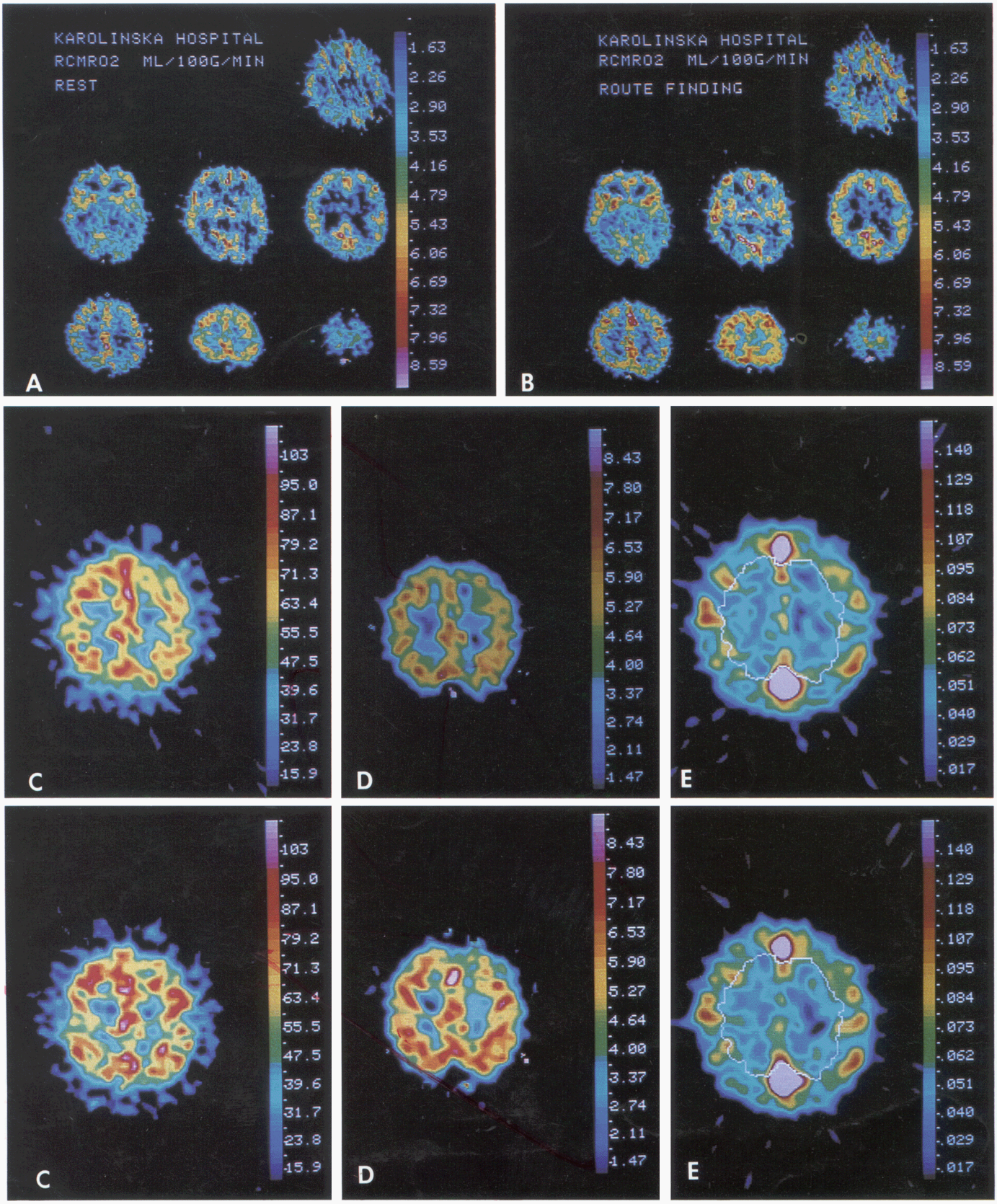

Figure 7. Changes in $rCMRO_2$, rCBF, and rCBV induced by thinking comprised of visual imagery. Each section is viewed from below (shown with the right side of the brain to the left). *A,* $rCMRO_2$ (in ml/100 gm/min) in a healthy young volunteer (14760) at rest (there are some detector artifacts in slice 1). *B,* While the volunteer was imagining walking a specific route. Note that $rCMRO_2$ increases in the prefrontal cortex, anterior neostriatum, thalamus, intraparietal and posterior superior parietal cortex. *C,* rCBF (in ml/100 gm/min) in slice 6 of another subject (14517) at

Table 5. Stereotaxic coordinates of the functional subdivisions mentioned in text and tables

Anterior cingular	2C4 2C5 3B4 3B5
Orbitofrontal	1A2 1A3 1A4 1A5 1A6 1A7
Gyrus rectus	1B4 1C4 1B5 1C5
Inf. frontal ant.	1B2 1B3 1B6 1B7 1C2 1C3 1C6 1C7
Inf. frontal mid.	2B2 2B7 2C2 2C7 3C2 3C7 3D1 3D8
Broca (inf. frontal post.)	2C2 2C7 3D1 3D8
Inf. frontal pole	2A4 2B4 2A5 2B5 3A4 3A5
Sup. frontal pole	4A4 4A5
Intermedial prefrontal ant.	2A2 2A3 2A6 2A7 3A2 3A3 3A6 3A7 3B2 3B7 4A3 4A6 4B2 4B7
Intermedial prefrontal post.	4C1 4C2 4C7 4C8 4D1 4D8
Midfrontal ant.	5B2 5B3 5B6 5B7
Midfrontal mid.	6C2 6C7
Midfrontal post.	5D2 5D7 6D2 6D7 6E2 6E7
Frontal eye fields	5D2 5D7 6E2 6E7
Sup. prefrontal ant.	4B4 4B5 5A4 5A5 5B4 5B5
Sup. prefrontal mid.	5C4 5C5 6B4 6B5
Sup. prefrontal post.	6C4 6C5 7C4 7C5
Supplementary motor	6D4 6D5 6E4 6E5 7D4 7D5 7E4 7E5
Premotor	7D2 7D3 7D6 7D7
Primary sensorimotor	4D1 4D8 4E1 4E8 5E1 5E8 6E1 6E2 6E7 6E8 6F4 6F5 7E2 7E7 7F4 7F5
Insula	2C3 2C6 2D2 2D7 2E2 2E7 3C2 3C3 3C6 3C7 3D2 3D7 3E2 3E7
Temporal lobe	1D1 1D2 1D7 1D8
Superior temporal	2D1 2D2 2D7 2D8 3E4 3E8 3F1 3F8
Midtemporal	1E1 1E8 2E1 2E8
Posterior inf. temporal	2F1 2F8 2G1 2G8 2H1 2H2 2H7 2H8
Parietotemporo-occipital	3B1 3B8 4G1 4G2 4G7 4G8
Lingual	2G3 2G6 2H3 2H6
Calcarine	3G3 3G4 3G5 3G6 3H4 3H5 3I4 3I5 4H4 4H5 4I4 4I5
Occipital inf.	2I3 2I4 2I5 2I6
Occipital lat.	3I2 3I3 3I6 3I7
Occipital sup.	4H2 4H7 4I2 4I3 4I6 4I7
Supplementary sensory	7G4 7G5
Superior parietal ant.	7F2 7F7
Intraparietal ant.	6F1 6F2 6F7 6F8
Intraparietal post.	6G2 6G7
Supramarginal	4F1 4F8 5F1 5F8
Angular	5G1 5G2 5G7 5G8
Superior parietal post. med.	5F4 5F5 5G4 5G5 6G4 6G5
Superior parietal post. lat.	5H3 5H4 5H6 5H7 6H2 6H3 6H4 6H5 6H6 6H7
Hippocampus	2F3 2F6 3F3 3F6
Caput caudatus	Atlas
Caudatus-putamen	Atlas
Putamen-pallidum	Atlas
Thalamus	Atlas
Cerebellum	Atlas

to incorrect timing of the arrival of isotope to the brain. The error was nonlinear. Since we sampled $Ca_{O_2}(t)$, $Ca_{CH_3F}(t)$, and the total number of coincidences from the brain every second, it was possible to reduce this error and achieve a fit between model and data that would have been impossible if the $Ca_{O_2}(t)$ and $Ca_{CH_3F}(t)$ had been measured from blood samples taken manually.

The rCBF was a linear factor in equation (2) and the rCBF

←

rest (*top*) and while imagining walking a specific route (*lower*). Note increases of rCBF in prefrontal and parietal fields. *D*, $rCMRO_2$ in slice 6 of subject 14517 at rest (*top*) and during mental route walking (*lower*). Note increases of $rCMRO_2$ in same fields as in *C*. *E*, rCBV (in ml/100 gm) of subject 14517 at rest (*top*) and during mental route walking (*lower*). Note increases of rCBV in the subarachnoid space outside the right frontal lobe, the left central region, and smaller increases outside the postparietal cortex.

also appeared as a linear factor and as an exponential value in equation (1). The use of a diffusion-limited tracer, as, for example, ^{15}O-labeled water, for the rCBF measurements would give $rCMRO_2$ values that were considerably lower than the present values. By the use of a freely diffusible tracer, such as $^{11}CH_3F$, the tissue flow and the input to the brain compartment can be accurately estimated. However since the egress of the metabolically produced ^{15}O-labeled water is diffusion-limited, the $rCMRO_2$ values are also sensitive to the brain:blood partition coefficient for water. The influence of a wrong partition coefficient for water becomes greater the longer the time of measurement, t_1–t_2, for determination of E is. In this study, we used a measured value of 0.80. For the present subjects, 50 and 90 sec measurements produced no difference in the calculated values of E.

The values for the rCBF in rest and the ratio of gray matter flow to white matter flow of 3.8:1 were in perfect agreement with blood flow measurements in animals and man obtained with other precise techniques (Reivich et al., 1969; Lassen, 1985). Our results for the mean $CMRO_2$ at rest were considerably higher than the value, 2.93 ± 0.37 ml/100 gm/min (mean ± SD), found by Mintun et al. (1984). These authors used ^{15}O-labeled water as flow tracer and manual sampling of the blood radioactivity. Sokoloff et al. (1955) used the Kety–Schmidt technique and found that the mean $CMRO_2$ of the brain in healthy young volunteers at rest was 3.97 ± 0.43 ml/100 gm/min. This was in perfect agreement with our value, 4.00 ± 0.50 ml/100 gm/min.

Relations between changes in rCBF, $rCMRO_2$, and rCBV caused by physiological brain work

Linear correlations between rCBF and $rCMRO_2$ in rest have been found earlier with 2 other methods of determining $rCMRO_2$ (Raichle et al., 1976; Baron et al., 1982). The new finding was that the same linear correlation existed during physiological activation of the brain. Since differentiation of this linear relation yielded a prediction of the rCBF increases that actually occurred in the physiologically working cortical fields and subcortical structures, this strongly indicated that the local rCBF is coupled dynamically to the local $rCMRO_2$. Since the intracerebral oxygen extraction E did not change during physiological brain work, the nerve cells (and glial cells) must extract the same fraction of the supplied oxygen and the increase of $rCMRO_2$ must be accomplished by means of an increase of supplied oxygen via the rCBF increase. The mechanisms that couple the rCBF to the neural metabolic rate are unknown.

The rCBF increase meant that an increased amount of blood was transported through the region per unit time. This increased transport did not result in any increase of the intracerebral rCBV. However, the rCBV increased in the subarachnoid space. The larger venules and the veins draining the cerebral cortex are located extracerebrally on the surface of the brain in the subarachnoid space. The subarachnoid cerebral veins, with their lack of muscular tone, often dilate as a response to an increased inlet (Penfield and Jasper, 1954). The increase in extracerebral rCBV might give rise to errors in the estimation of $rCMRO_2$ in PET measurements with limited spatial resolution. If extracerebral venules and veins are included in the sampling of regional data, the regional oxygen extraction fraction E will decrease if the volume of these veins increases. An increase of the cerebral blood volume in subjects performing psychological tests has previously been found by Risberg and Ingvar (1968).

Pattern of $rCMRO_2$ changes during mental activity

The cortical metabolic increases were organized in fields, each extending over 2–10 cm^3 of cortex. Field increase of rCBF during physiological activity have been observed in many studies (for a review, see Roland, 1985a, b). The present data support the field-activation hypothesis (Roland, 1985a), which states that the cerebral cortex participates in physiological brain work in awake human subjects by increasing the metabolism in multiple cortical fields, each a few square centimeters (or a few cubic centimeters) in size. We found no decreases in $rCMRO_2$ during mental activity. The brain, therefore, does not compensate for the $rCMRO_2$ increases in activated structures with $rCMRO_2$ decreases in other, inactive regions.

A natural first question is whether the $rCMRO_2$ increases were caused by neurons participating in the creation of the specific mental activity. Immediately prior to the arrival of the isotope in the brain, the subjects took a deep inhalation. With the exception of the increase in the left superior prefrontal cortex, the distribution of metabolic increases that appeared in the present study was entirely different from those seen in an earlier study in which subjects also inhaled an isotope (Roland et al., 1982). Since the superior prefrontal cortex on the left is activated in many tasks not preceded by any inhalations (for a review, see Roland, 1984, 1985b), it is unlikely that any of the present metabolic increases would be related to the inhalation procedure. Furthermore, the inhalation procedure was exactly the same in rest as during mental activity.

Since there was an increase in $rCMRO_2$ in the left frontal eye field and another $rCMRO_2$ increase appeared in the right cerebellar hemisphere, one might think that this was a sign of motor activity. We did not record eye movements, but mental activity is often accompanied by involuntary lateral movements of the eyes (Day, 1964; Bakan and Svorad, 1969). Furthermore, the subjects reported that, when having recalled a scene, they looked around in the image space, searching for crossroads and scrutinizing the houses and vegetation, focusing their attention on particular features in the retrieved image space. Voluntary eye movements in subjects with closed eyes increases rCBF in the frontal eye fields, the transition zone between the supplementary motor area and the posterior prefrontal cortex and in the cerebellar vermis region (Melamed and Larsen, 1979; Fox et al., 1985a, b). However, the magnitudes of rCBF increases in the frontal eye fields have been more closely related to the direction of attention than to the frequency of eye movements (Roland et al., 1981; Roland, 1982). We cannot, however, exclude the possibility that the activity in the left frontal eye field and the posterior superior prefrontal cortex was in part due to eye movements. These movements might have been task-related, but of course not directed towards external targets. However, it is very unlikely that the remaining $rCMRO_2$ increases were related to eye movements. This applies also to the neostriatal increases in $rCMRO_2$ (Alexander and DeLong, 1985; DeLong et al., 1985).

None of the subjects showed any signs of extraorbital muscle activity. Extraorbital muscle activity would be expected to increase the $rCMRO_2$ in the motor areas of the cortex, the basal ganglia, the ventral thalamus, and the parasagittal part of the anterior lobe of cerebellum (Snider, 1950; Roland et al. 1982; Fox et al., 1985b). The increase of $rCMRO_2$ in the lateral cerebellum consequently was most likely related to nonmotor activity. Many of the activated prefrontal areas project to this part of neocerebellum (Sasaki, 1979).

The motor areas and primary sensory areas had no changes in $rCMRO_2$. In the absence of any detectable extraorbital muscular contractions, any changes in position of the limbs and body, or any visual input, it is unlikely that the afferent sensory fiber activity would change systematically (Vallbo et al., 1979). Moreover, the slight noise from the cooling fans of the PET camera did not change between rest and mental activity. It is thus unlikely that any of the measured $rCMRO_2$ increases were due to treatment of incoming sensory information. Thus, with the possible exceptions of $rCMRO_2$ increases in the left frontal eye field and the posterior superior prefrontal cortex, we must conclude that the observed $rCMRO_2$ increases were most likely related exclusively to intrinsic brain activity.

Because the $rCMRO_2$ increases were of different magnitudes in different brain structures, and because the primary sensory areas, the motor areas, and several other cortical areas and subcortical structures did not increase their $rCMRO_2$, the observed $rCMRO_2$ increases could not have been produced by a state of general arousal.

When the subjects' imagined walk was stopped, all had arrived at a geographical point located in the correct direction. They were able to describe landmarks of the route they took. This demonstrated that they had all retrieved images from their memory, and analyzed and operated on these images according to the algorithm specified in the instructions. Thus, the increases of $rCMRO_2$ in at least some cortical fields and subcortical structures must have been related to the retrieval of images from memory, and the analysis and operations on these images. Every subject had clear (more than 15%) increases of $rCMRO_2$ in the right middle superior prefrontal cortex, the whole intermediate prefrontal cortex on both sides, the right anterior and middle midfrontal cortex, the left posterior midfrontal cortex, and bilateral increases in the posterior intraparietal cortex, the posterior superior parietal cortex, neostriatum, and posterior thalamus. Since the task was identical for all subjects, and since all subjects during the period in which these increases in $rCMRO_2$ were measured retrieved images from memory, and analyzed and operated upon these images, the most natural conclusion is that the listed structures contained neurons that increased their oxidative metabolism because they participated in the task. Roland and Friberg (1985), who used the same paradigm, applied a significance limit of 0.01 to their results. If this limit is applied in Tables 3 and 4, there is perfect agreement in the cortical areas showing increases of rCBF between the 2 studies. Such reproducibility would not be expected if the $rCMRO_2$ increases in some areas were signs of non-task-related activity.

Functional significance of the $rCMRO_2$ increases

The functional contribution of the activated neuron populations to the retrieval of visual information from memory, the representations of the retrieved images, and the operations on the retrieved information is not apparent from the present study. Such a functional analysis must be based on comparisons with all previous functional mapping studies. The superior prefrontal regions have been activated totally independently of task-related algorithms, sensory input, or motor output in many previous tasks that did not contain any elements of memory retrieval or visual imagery. These areas are assumed to participate in the (intrinsic) organization of brain work (for a review, see Roland, 1985b).

Operations that require knowledge of relations in extrapersonal space are reported to increase the rCBF in the midfrontal and anterior intermediate prefrontal areas, the frontal eye fields, the superior parietal cortex, and the intraparietal region (Roland et al., 1980; Motter and Mountcastle, 1981; Andersen et al., 1985). In the macaque, there are heavy anatomical connections between the lateral prefrontal cortex, including the frontal eye fields, and area 7 in the posterior parietal cortex, especially around the intraparietal sulcus (Pandya et al., 1971; Barbas and Mesulam, 1981). The co-activation of these cortical areas in the present study was thus in accordance with these previous findings and the subjects' operations in their imagined 3-dimensional visual space.

The anterior part of the caudate putamen increased the metabolism as well. In the macaque, this part of neostriatum receives its afferents from the prefrontal cortex. The further handling of this prefrontal input seems segregated from the input from motor areas (Nauta and Mehler, 1966; Kuo and Carpenter, 1973; DeLong et al., 1983). Apart from possible involuntary eye movements, there was no motor activity accompanying the thinking. None of the motor areas showed any $rCMRO_2$ increases. The $rCMRO_2$ increase in the anterior neostriatum thus could hardly be from neurons participating in motor activity (Alexander and DeLong, 1985; DeLong et al., 1985); it was probably a sign of activity in neurons transforming information coming from the activated prefrontal cortex.

Despite the fact that the task was a recall of visual information, we observed no changes of the $rCMRO_2$ in hippocampus and amygdala. In the stereotaxic positioning of the head that we used, only a small cross section of the hippocampus, which was subject to partial volume effect, was seen. The amygdala is an even smaller structure, which was also subject to partial volume effect. The left insular $rCMRO_2$ increase ($p = 0.005$; Table 4), however, could be related to activation of paralimbic structures.

One might ask if any of the metabolically active neuron populations were representing the retrieved visual–spatial images. The metabolism did not change in the calcarine cortex and the immediately surrounding cortex. The retrieval and analysis of the 3-dimensional spatial images thus did not require any contribution from the primary visual cortex and the immediate visual-association areas. The $rCMRO_2$ increased moderately in the superior occipital cortex and the posterior inferior temporal cortex. Since the subjects did not receive any stimuli, the metabolic work of these neuron populations must have been initiated by the brain itself via intercortical or subcortical connections. Comparably higher increases in rCBF and glucose consumption in these areas appeared in studies in which subjects were analyzing visual information from the outside world for details (Phelps et al., 1981; Roland and Skinhöj, 1981; Mazziotta et al., 1982; see also Macko and Mishkin, 1985). These areas have not been activated when nonvisual information has been analyzed in the brain during mental calculations or motor tasks (Roland et al., 1980, 1981, 1982, 1985; Mazziotta et al., 1982, 1985; Roland and Friberg, 1985). They are probably remote visual-association areas.

All subjects reported that, while performing the task, they saw visual images nearly continuously. It was reasonable, therefore, to assume that the cortical areas that had been most active for the longest periods during the PET measurement would have the highest metabolic increases. Most of the processing time during the task must have been spent on retrieval of images and analysis of these images. By far the strongest increases of $rCMRO_2$ appeared in the superior posterior medial and lateral parietal cortices. In another study, in which subjects were requested to

recall the appearance of items in their living room, the right superior posterior lateral parietal area alone was activated from the parietal and occipital cortex (Roland et al., 1985). The homologs of the superior posterior parietal lateral and medial area are not known for other primates. But it is said that in the macaque, the visual-association areas in the temporal lobe process information about physical qualities of objects, whereas the visual areas in the parietal lobe process spatial information (Macko and Mishkin, 1985). We suggest, therefore, that the retrieved visual images are represented in the active fields in the superior posterior parietal cortex. It is impossible to say whether the images are represented in the lateral or the medial area, since the medial area has not previously been metabolically explored. The superior posterior parietal areas are probably visual-association areas that provide fully reconstructed memorized scenes, i.e., scenes that are complete in color, space representation, and details. The roles of the other, moderately activated remote visual-association areas could then have been to participate in transformations of the memorized information represented in the superior parietal fields.

Since the pulvinar is by far the largest structure in the human posterior thalamus, the posterior thalamic $rCMRO_2$ increase must, at least in part, have originated from the pulvinar. This structure receives afferents from the lateral prefrontal cortex and projects to the superior posterior medial parietal cortex, among other parietal areas (van Buren, 1974; Trojanovski and Jacobson, 1976; Kievit and Kuypers, 1977). Electrical stimulation of the pulvinar can cause transient defects in recall (Ojeman, 1974). The present finding of a marked $rCMRO_2$ increase in the posterior thalamus thus was in accordance with the hypothesis that the pulvinar participates in the retrieval of visual images from memory.

References

Alexander, G. E., and M. R. DeLong (1985) Microstimulation of the primate neostriatum. I. Physiological properties of striatal microexcitable zones. J. Neurophysiol. *53:* 1401–1416.

Andersen, R. A., G. K. Essick, and R. M. Siegel (1985) Encoding of spatial location by posterior parietal neurons. Science *230:* 456–458.

Bakan, P., and D. Svorad (1969) Resting EEG alpha and asymmetry of reflective lateral eye movements. Nature *223:* 975–976.

Barbas, H., and M.-M. Mesulam (1981) Organization of afferent input to subdivisions of area 8 in the rhesus monkey. J. Comp. Neurol. *200:* 407–431.

Baron, G. C., P. Lebrun-Grandie, P. Collard, C. Crouzel, G. Mestelan, and M. G. Bousser (1982) Noninvasive measurement of blood flow, oxygen consumption and glucose utilization in the same brain regions in man by positron emission tomography. J. Nucl. Med. *23:* 391–399.

Bergström, M., J. Boethius, L. Eriksson, T. Greitz, T. Ribbe, and L. Widén (1981) Head fixation device for reproducible positron alignment in transmission CT and positron emission tomography. J. Comput. Assist. Tomogr. *5:* 136–141.

Bergström, M., J. Litton, L. Eriksson, C. Bohm, and G. Blomqvist (1982) Determination of object contour from projections for attenuation correction in cranial positron emission tomography. J. Comput. Assist. Tomogr. *6:* 365–372.

Bohm, C., T. Greitz, D. Kingsley, B. M. Berggren, and L. Olsson (1985) A computerized individually variable stereotaxic brain atlas. In *The Metabolism of the Human Brain Studied with Positron Emission Tomography,* T. Greitz, D. H. Ingvar, and L. Widen, eds., pp. 85–91, Raven, New York.

Carter, C. C., J. O. Eichling, D. O. Davis, and M. M. Ter-Pogossian (1972) Correlation of regional cerebral blood flow with regional oxygen uptake using 15-O method. Neurology *22:* 755–762.

Davis, F. E., K. Kenyon, and J. Kirk (1953) A titrimetric method for determining the water content of human blood. Science *118:* 276–277.

Day, M. E. (1964) An eye movement phenomenon relating to attention, thought and anxiety. Percept. Mot. Skills *19:* 433–446.

DeLong, M. R., A. P. Georgopoulos, and M. D. Crutcher (1983) Cortico-basal ganglia relations and coding of motor performance. In *Neural Coding of Motor Performance,* J. Massion, J. Paillard, W. Schultz, and M. Wiesendanger, eds., pp. 30–40, Springer, Heidelberg.

DeLong, M. R., M. D. Crutcher, and A. P. Georgopoulos (1985) Primate globus pallidus and subthalamic nucleus. J. Neurophysiol. *53:* 530–543.

Fox, P. T., and M. E. Raichle (1986) Focal physiological uncoupling of cerebral blood flow and oxidative metabolism during somatosensory stimulation in human subjects. Proc. Natl. Acad. Sci. USA *83:* 1140–1144.

Fox, P. T., J. E. Fox, M. E. Raichle, and R. M. Burde (1985a) The role of cerebral cortex in the generation of voluntary saccades: A position emission tomographic study. J. Neurophysiol. *54:* 348–369.

Fox, P. T., M. E. Raichle, and W. T. Thach (1985b) Functional mapping of the human cerebellum with positron emission tomography. Proc. Natl. Acad. Sci. USA *82:* 7462–7466.

Frackowiak, R. S. J., G.-L. Lenzi, T. Jones, and J. D. Heather (1980) Quantitative measurement of regional cerebral blood flow and oxygen metabolism in man using 150 and positron emission tomography: Theory, procedure, and normal values. J. Comput. Assist. Tomogr. *4:* 727–736.

Friedman, P. A., A. H. Kappelman, and S. Kaufman (1972) Partial purification and characterization of tryptophan hydroxylase from rabbit hind brain. J. Biol. Chem. *247:* 4165–4173.

Greenberg, F., P. Hand, A. Sylvestro, and M. Reivich (1979) Localized metabolic flow couple during functional activity. Acta Neurol. Scand. (Suppl.) *72:* 12–14.

Greitz, T. (1956) A radiological study of the brain circulation by rapid serial angiography of the carotid artery. Acta Radiol. (Suppl.) *140:* 1–123.

Greitz, T., D. H. Ingvar, and L. Widen (1985) *The Metabolism of the Human Brain Studied with Positron Emission Tomography,* p. 507, Raven, New York.

Grubb, R. L., M. E. Raichle, C. S. Higgins, and J. O. Eichling (1978) Measurement of regional cerebral blood volume by emission tomography. Ann. Neurol. *4:* 322–328.

Huang, S.-C., D. G. Feng, and M. E. Phelps (1986) Model dependency and estimation reliability in measurement of cerebral oxygen rate with oxygen-15 and dynamic positron emission tomography. J. Cerebr. Blood Flow Metab. *6:* 105–119.

Kennedy, C., M. H. Des Roisiers, O. Sakurada, M. Shinohara, M. Reivich, J. W. Jehle, and L. Sokoloff (1976) Metabolic mapping of the primary visual system of the monkey by means of the autoradiographic ^{14}C-deoxyglucose technique. Proc. Natl. Acad. Sci. USA *73:* 4230–4234.

Kennedy, C., M. Miyaoka, S. Suda, K. Macko, C. Jarvis, M. Mishkin, and L. Sokoloff (1980) Local metabolic responses in brain accompanying motor activity. Trans. Am. Neurol. Assoc. *105:* 310.

Kety, S. S. (1951) The theory and applications of the exchange of inert gas at the lungs and tissues. Pharmacol. Rev. *3:* 1–41.

Kievit, J., and H. G. J. M. Kuypers (1977) Organization of the thalamo-cortical connexions to the frontal lobe in the rhesus monkey. Exp. Brain Res. *29:* 299–322.

Koeppe, R. A., J. E. Holden, and W. R. Ip (1985) Performance of parameter estimation techniques for the quantification of local cerebral blood flow by dynamic positron computed tomography. J. Cerebr. Blood Flow Metab. *5:* 224–234.

Kuo, J.-S., and M. B. Carpenter (1973) Organization of pallidothalamic projections in the rhesus monkey. J. Comp. Neurol. *151:* 201–236.

Lassen, N. A. (1985) Editorial: Normal average value of cerebral blood flow in younger adults is 50 ml/100 g/min. J. Cerebr. Blood Flow Metab. *5:* 347–349.

Litton, J.-E., M. Bergström, L. Eriksson, C. Bohm, and G. Blomquist (1984) Performance study of the PC384 positron camera system for emission tomography of the brain. J. Comput. Assist. Tomogr. *8:* 74–87.

Lubbers, D. W. (1974) Das O_2-Versorgungssystem der Warmblutorgane. In *Jahrbuch der Max Planck Gesellshaft zur Förderung der Wissenschaften,* pp. 87–112, Göttingen, FRG.

Macko, K. A., and M. Mishkin (1985) Metabolic mapping of higher-order visual areas on the monkey. In *Brain Imaging and Brain Function,* L. Sokoloff, ed., pp. 73–86, Raven, New York.

Mazziotta, J. C., M. E. Phelps, R. E. Carson, and D. E. Kuhl (1982) Tomographic mapping of human cerebral metabolism: Auditory stimulation. Neurology *32:* 921–937.

Mazziotta, J. C., M. E. Phelps, and J. A. Wapenski (1985) Human cerebral motor system metabolic responses in health and disease. J. Cerebr. Blood Flow Metab. (Suppl. 1)*5:* S213–S214.

Melamed, E., and B. Larsen (1979) Cortical activation pattern during saccadic eye movements in humans: Localization by focal cerebral blood flow increases. Ann. Neurol. *5:* 79–88.

Mintun, M. A., M. E. Raichle, W. R. W. Martin, and P. Herscowitch (1984) Brain oxygen utilization measured with ^{15}O radiotracers and positron emission tomography. J. Nucl. Med. *25:* 177–187.

Motter, B. C., and V. B. Mountcastle (1981) The functional properties of the light sensitive neurons of the posterior parietal cortex studied in waking monkeys: Foveal sparing and opponent vector organization. J. Neurosci. *1:* 1218–1235.

Nauta, W. J. H., and W. R. Mehler (1966) Projections of the lentiform nucleus in the monkey. Brain Res. *1:* 3–42.

Nilsson, J. L. G., S. Stone-Elander, E. Ehrin, B. Garmelius, and P. Johnström (1985) ^{11}C-labeled compounds for the study of cerebral blood volume, blood flow, and energy metabolism. In *The Metabolism of the Human Brain Studied with Positron Emission Tomography,* T. Greitz, D. H. Ingvar, and L. Widen, eds., pp. 107–122, Raven, New York.

Ojeman, G. A. (1974) Speech and short term verbal memory alterations evoked from stimulation in pulvinar. In *The Pulvinar–LP Complex,* I. S. Cooper, M. Riklan, and P. Rakic, eds., pp. 173–184, Charles Thomas, Springfield, IL.

Oldfield, R. C. (1971) The assessment and analysis of handedness: The Edinburgh inventory. Neuropsychologia *9:* 97–113.

Olesen, J., O. Paulson, and N. A. Lassen (1971) Regional cerebral blood flow in man determined by the initial slope of the clearance of intraarterially injected 133Xe. Stroke *2:* 519–540.

Pandya, D. N., P. Dye, and N. Butters (1971) Efferent cortico-cortical projections of the prefrontal cortex in the rhesus monkey. Brain Res. *14:* 49–65.

Penfield, W., and H. Jasper (1954) *Epilepsy and Functional Anatomy of the Human Brain,* Little, Brown, Boston, MA.

Phelps, M. E., D. E. Kuhl, J. C. Mazziotta (1981) Metabolic mapping of the brain's response to visual stimulation: Studies in humans. Science *211:* 1445–1448.

Phelps, M. E., J. C. Mazziotta, and H. R. Schelbert (1986) *Positron Emission Tomography and Autoradiography,* Raven, New York.

Raichle, M. E., R. L. Grubb, M. H. Gado, J. O. Eichling, and M. M. Ter-Pogossian (1976) Correlation between regional cerebral blood flow and oxidative metabolism. Arch. Neurol. *33:* 523–526.

Reivich, M., J. Jehle, L. Sokoloff, and S. Kety (1969) Measurement of regional cerebral blood flow with antipyrine-^{14}C in awake cats. J. Appl. Physiol. *27:* 296–300.

Reivich, M., A. Alavi, J. H. Greenberg, J. Fowler, D. Christman, R. MacGregor, S. C. Jones, J. London, C. Shiue, and Y. Yonekura (1982) Use of 2-deoxy-d^{11}C-glucose for the determination of local cerebral glucose metabolism in humans: Variation within and between subjects. J. Cerebr. Blood Flow Metab. *2:* 307–319.

Risberg, J., and D. H. Ingvar (1968) Regional changes in the cerebral blood volume during mental activity. Exp. Brain Res. *5:* 72–78.

Roland, P. E. (1982) Cortical regulation of selective attention. J. Neurophysiol. *48:* 1059–1078.

Roland, P. E. (1984) Metabolic measurements of the working frontal cortex in man. Trends Neurosci. *7:* 403–435.

Roland, P. E. (1985a) Application of imaging of brain blood flow to behavioral neurophysiology: The cortical field activation hypothesis. In *Brain Imaging and Brain Function,* L. Sokoloff, ed., pp. 87–104, Raven, New York.

Roland, P. E. (1985b) Cortical organization of voluntary behavior in man. Hum. Neurobiol. *4:* 155–167.

Roland, P. E., and L. Friberg (1985) Localization of cortical areas activated by thinking. J. Neurophysiol. *53:* 1219–1243.

Roland, P. E., and E. Skinhöj (1981) Extrastriate visual areas activated during visual discrimination in man. Brain Res. *222:* 166–171.

Roland, P. E., E. Skinhöj, N. A. Lassen, and B. Larsen (1980) Different cortical areas in man in organization of voluntary movements in extrapersonal space. J. Neurophysiol. *45:* 1139–1151.

Roland, P. E., E. Skinhöj, and N. A. Lassen (1981) Focal activations of human cerebral cortex during auditory discrimination. J. Neurophysiol. *45:* 1139–1151.

Roland, P. E., E. Meyer, T. Shibasaki, Y. L. Yamamoto, and C. J Thompson (1982) Regional cerebral blood flow changes in cortex and basal ganglia during voluntary movements in normal human volunteers. J. Neurophysiol. *48:* 467–480.

Roland, P. E., L. Friberg, N. A. Lassen, and T. S. Olsen (1985) Regional cortical blood flow changes during production of fluent speech and during conversation. J. Cerebr. Blood Flow Metab. (Suppl. 1)*5:* S205–S206.

Rushmer, R. F. (1976) *Cardiovascular Dynamics,* 4th Ed., p. 8, Saunders, Philadelphia, PA.

Sasaki, K. (1979) Cerebro-cerebellar interconnections in cats and monkeys. In *Cerebro-Cerebellar Interactions,* J. Massion and K. Sasaki, eds., pp. 105–124, Elsevier, Amsterdam.

Siggaard-Andersen, O. (1977) Experiences with a new direct-reading oxygen saturation photometer using ultrasound for hemolyzing the blood. Scand. J. Clin. Lab. Invest. (Suppl. 146)*37:* 45–50.

Silver, I. A. (1966) The measurement of oxygen in tissues. In *Oxygen Measurements in Blood and Tissues and their Significance,* J. P. Payne and D. W. Hill, eds., pp. 299–312, Churchill, London.

Snider, R. S. (1950) Recent contributions to the anatomy and physiology of the cerebellum. Arch. Neurol. Psychiatry *64:* 196–219.

Sokoloff, L., R. Mangold, R. L. Wechsler, C. Kennedy, and S. Kety (1955) The effect of mental activity on cerebral circulation and metabolism. J. Clin. Invest. *34:* 1101–1108.

Stone-Elander, S., P. Roland, L. Eriksson, J.-E. Litton, P. Johnström, and L. Widén (1986) The preparation of ^{11}C-labelled fluoromethane for the study of regional cerebral blood flow using positron emission tomography. Eur. J. Nucl. Med. *12:* 236–239.

Talairach, J., G. Szikla, P. Tournoux, A. Prossalentis, M. Bordas-Ferrer, L. Covello, M. Iacob, and E. Mempel (1967) *Atlas d'Anatomie Stereotaxique du Telencephale,* Masson, Paris.

Thews, G. (1960) Ein Verfahren zur Bestimmung des O_2-Diffusionskoefficienten, der O_2-Leitfähigkeit und des O_2-Löslichkeitskoefficienten im Gehirngewebe. Pfluegers Arch. *217:* 227–244.

Torack, R. M., H. Alcala, M. Gado, and R. Burton (1976) Correlative assay of computerized cranial tomography (CCT), water content and specific gravity in normal and pathological postmortem brain. J. Neuropathol. Exp. Neurol. *35:* 385–392.

Trojanovski, J. O., and S. Jacobson (1976) Areal and laminar distribution of some pulvinar cortical efferents in rhesus monkey. J. Comp. Neurol. *169:* 371-391.

Vallbo, Å. B., K. E. Hagbarth, H. E. Torebjörk, and B. G. Wallin (1979) Somatosensory, proprioceptive, and sympathetic activity in human peripheral nerves. Physiol. Rev. *59:* 919–957.

van Buren, J. M. (1974) Anatomic studies of pulvinar in humans. In *The Pulvinar–LP Complex,* I. S. Cooper, M. Riklan, and P. Rakic, eds., pp. 67–79, Charles Thomas, Springfield, IL.

van Slyke, D. D., R. A. Phillips, V. P. Dole, P. B. Hamilton, R. M. Archibald, and J. Plazin (1950) Calculation of hemoglobin from blood specific gravities. J. Biol. Chem. *183:* 349–351.